ISSN 2599-3496 print
ISSN 2614-2376 online
Volume 8, Number 1 2025

INTERNATIONAL JOURNAL of OIL PALM

By Indonesian Oil Palm Society

Oil Palm Plantation Fund Management Agency

Palm oil is Indonesia's most strategic commodity. It has significant contribution to the economy, creates million employments and boosts regional development. BPDPKS, established in 2015, is to support the development and suistainability of Indonesian Palm Oil sector through prudent, transparent, and accountable management of funds. As the fund management agency, BPDPKS ensures "from palm oil to palm oil" principle to be implemented in every program.

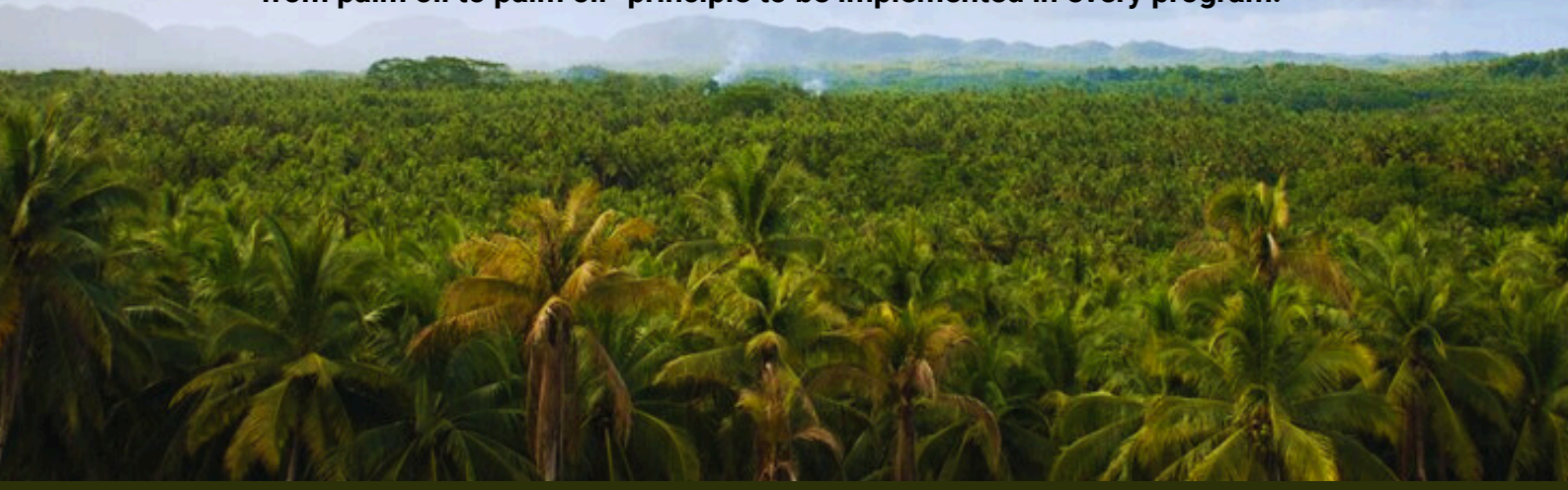

Main Area of Fund Disbursement

(Based on Presidential Regulation No. 61/2015)

- Food Security, Downstream Market Development and Biodiesel Supply
- Replanting
- Facilities, Infrastructures, and Farmers Empowerment
- Human Resources Development
- Research and Development
- Promotion and Advocacy

Current Fund Disbursement Program

Biodiesel Supply

Support Biodiesel Mandatory Program to strengthen Indonesia energy security and the use of renewable energy.

Replanting Program

Support replanting program for smallholders farmers to increase productivity and welfare and to avoid land use, land-use change and forestry (LULUCF).

Farmers Training and Development

A human resources development program in palm oil sector through training, education, counseling, accompainment and facilitation.

Research and Development

Support the research and development initiatives in palm oil sector to increase productivity, sustainability and product development.

Promotion and Advocacy

Support the Goverment, Industry and relevant stakeholders to increase positive public awareness on palm oil sector and its products.

Facilities and Infrastructure Support

Support palm oil smallholder farmers in improving its facilities and infrastructure to increase productivity.

Gedung Surachman Tjokrodisurjo Lt 1
Jl. Medan Merdeka Timur No. 16, Gambir, Jakarta Pusat
E : bpdpsawit@bpdp.or.id
W : www.bpdp.or.id

Badan Pengelola Dana Perkebunan (BPDP)

INTERNATIONAL JOURNAL of OIL PALM

Volume 8, Number 1, 2025

ISSN: 2599-3496 print
ISSN: 2614-2376 online

INTERNATIONAL JOURNAL of OIL PALM
ISSN: 2599-3496 print
ISSN: 2614-2376 online

Volume 8, Number 1, 2025
Page 1–14
DOI: 10.35876/ijop.v8i1.138

Sea Level Rise Impacts on Coastal Oil Palm Plantations

Jogi Panggabean*, Julian Kurnia, Teuku Shaumul

Marine Science Program, Faculty of Fisheries and Marine Science,
Universitas Padjajaran

ABSTRACT

Indonesia's coastal oil palm plantations face unprecedented threats from accelerating sea level rise, with regional rates of 4–5 mm year^{-1} significantly exceeding global averages. This study presents the first comprehensive satellite-based assessment of sea level rise impacts on coastal oil palm vulnerability, focusing on Dumai City, Riau Province. We utilized five primary datasets spanning from 2020–2024: Landsat 8/9 and Sentinel-2 imagery for plantation mapping, SRTM DEM for topographic analysis, satellite altimetry for sea level measurements, and ground truth data for validation. Cross-wavelet analysis revealed an exceptionally strong negative correlation (r = -0.857) between sea level anomalies and coastal land cover changes, with a 30-day lag period indicating plantation ecosystem response time. NDVI trend analysis showed significant vegetation decline (-0.072 NDVI/year) over the study period, with plantation health deteriorating from optimal conditions in 2020 (mean NDVI: 0.608) to critical levels by 2024 (mean NDVI: 0.335). Land cover change detection revealed extensive palm oil expansion (+4,848 ha, +26.3%) occurring through conversion of natural forest (-3,114 ha, -22.8%) and mangrove ecosystems (-1,300 ha, -19.5%). Results reveal that 78% of coastal oil palm plantations are located within 5 km of shoreline on low-lying areas with elevations below 3 meters above sea level. The vulnerability assessment identified 2,847 hectares (64% of total coastal plantations) as highly vulnerable to inundation and saltwater intrusion, representing USD 12.3 million in annual production value at risk.

Keywords: Climate adaptation, coastal vulnerability, NDVI trend, remote sensing, satellite altimetry

INTRODUCTION

Indonesia's oil palm industry produces 47% of global palm oil supply and contributes significantly to the national economy, yet faces increasing vulnerability to climate change impacts, particularly sea level rise in coastal regions (BPS 2020; Danylo *et al.* 2021). The country's oil palm cultivation has expanded to over 16 million hectares, with substantial portions located in low-lying coastal provinces where plantation development concentrated on coastal peatlands inherently susceptible to both subsidence and sea level rise (Descals *et al.* 2019; Xu *et al.* 2020). Riau Province accounts for 2.4 million hectares of oil palm plantations, representing 20% of national production, with over 80% established on coastal peatlands experiencing ongoing subsidence due to drainage required for cultivation (Sumarga *et al.* 2016).

The intersection of oil palm cultivation and coastal vulnerability creates complex challenges for sustainable agricultural development. Recent studies have documented the interconnected impacts of

*Corresponding author:
Marine Science Program, Faculty of Fisheries and Marine Science
Universitas Padjajaran 40132
Email: jogipanggabeann@gmail.com

peatland drainage, subsidence, and coastal flooding on oil palm production systems (Hooijer *et al.* 2012; Sumarga *et al.* 2016). Drainage required for oil palm cultivation on peatlands causes progressive soil subsidence, with rates reaching 2.8 cm year^{-1} in newly drained areas, progressively increasing flood risks and threatening plantation viability as oil palm is highly sensitive to waterlogged conditions (Hooijer *et al.* 2012). Furthermore, coastal peatland degradation increases vulnerability to tidal flooding and saltwater intrusion, with formerly protective coastal ecosystems now contributing to agricultural vulnerability rather than providing natural protection (Hastuti *et al.* 2022).

Despite these methodological advances, no comprehensive study has systematically assessed the vulnerability of Indonesian coastal oil palm plantations to sea level rise using integrated satellite remote sensing approaches. This knowledge gap is particularly critical given the rapid pace of both sea level rise and oil palm expansion in Indonesian coastal areas, with some coastal areas experiencing combined land subsidence and sea level rise rates exceeding 10 cm year^{-1} (Lumban-Gaol *et al.* 2024).

MATERIALS AND METHODS

This study focuses on Dumai City, Riau Province, Sumatra, Indonesia (1°40'N –1°45'N, 101°25'E–101°30'E), which serves as a representative case study for coastal oil palm vulnerability assessment (Figure 1). Dumai City was selected due to its strategic importance as a major palm oil export hub, with approximately 80% of the municipal area consisting of coastal peatlands where extensive oil palm cultivation has been established over the past three decades (Siegel *et al.* 2019). The study area encompasses approximately 1,623 km² of coastal lowlands with elevations ranging from 0 to 15 meters above sea level, characterized by extensive peat deposits with depths reaching 3–8 meters (Baum *et al.* 2007).

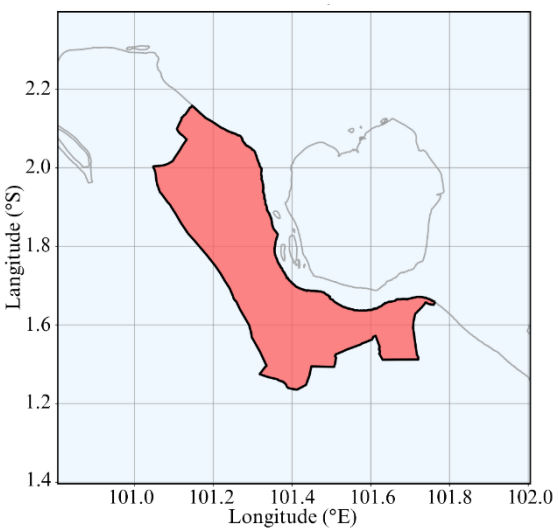

Figure 1 Study area location map showing Dumai City, Riau Province, Indonesia with coastal zone boundaries.

The coastline extends approximately 45 km along the Malacca Strait, featuring a complex mosaic of oil palm plantations, natural mangrove remnants, aquaculture ponds, and urban development. Dumai experiences a tropical humid climate with annual precipitation of approximately 2,500 mm and mean temperatures of 26–28 °C throughout the year, conditions optimal for oil palm cultivation but creating challenges for drainage management on peat soils (Siegel *et al.* 2019). The area is influenced by semi-diurnal tides with ranges of 1.5–3.5 meters, creating extensive intertidal zones that directly interact with plantation drainage systems.

Data Sources

This research utilized five comprehensive datasets spanning 2020–2024. Landsat 8/9 Optical Imagery was obtained from the United States Geological Survey (USGS) Earth Explorer platform, with Landsat Collection 2 Level-2 Surface Reflectance products selected for consistent atmospheric correction (Vermote *et al.* 2016). A total of nine cloud-free images were acquired on specific dates: 2020-10-18, 2021-02-23, 2021-06-15, 2021-07-17, 2021-08-02, 2023-06-13, 2024-07-25, 2024-09-19, and 2024-12-16.

Sentinel-2 Multispectral Imagery was downloaded from the European Space Agency's Copernicus Open Access Hub, utilizing Level-2A Surface Reflectance products providing enhanced 10-meter spatial resolution (Drusch *et al.* 2012).

Sea level altimetry data was obtained from the Copernicus Marine Environment Monitoring Service (CMEMS) Multi-Mission Altimeter Satellite Gridded Sea Level Anomalies dataset, providing daily mean sea level anomalies at 0.125° spatial resolution for the Malacca Strait region (IPCC 2021). Digital Elevation Model data from the Shuttle Radar Topography Mission (SRTM) at 30-meter resolution was utilized following the vegetation correction methodology of O'Loughlin *et al.* (2016). Ground truth data for classification accuracy assessment contained 609 reference points distributed across different plantation types, ages, and environmental conditions.

Data Processing and Analysis

All satellite imagery processing was conducted using open-source software including QGIS 3.28 and Python-based libraries (GDAL, Rasterio, NumPy) to ensure reproducibility (Hansen *et al.* 2013). Landsat images were atmospherically corrected using the Land Surface Reflectance Code (LaSRC) algorithm, which accounts for atmospheric scattering effects in tropical coastal environments (Vermote *et al.* 2016). Geometric correction was systematically applied to ensure precise co-registration between multi-temporal images using ground control points identified from stable infrastructure features. Oil palm plantations were mapped through systematic visual interpretation of Sentinel-2 imagery combined with automated vegetation index analysis, following established criteria for plantation identification including regular geometric planting patterns, characteristic canopy texture, and spectral properties (Descals *et al.* 2019; Nurmasari and Wijayanto 2021). Four primary land cover classes were defined: oil palm plantations (subdivided into young 0–5 years and mature >5 years), natural forest and mangroves, other agriculture and bare land, and water bodies.

Normalized Difference Vegetation Index (NDVI) was calculated from all available imagery using the standard formula NDVI = (NIR - Red) / (NIR + Red), where NIR represents near-infrared reflectance and Red represents red wavelength reflectance (Xu *et al.* 2021). A comprehensive dekadal analysis was implemented covering 180 dekads (36 dekads per year × 5 years) from 2020–2024, with temporal interpolation applied to fill data gaps using spline interpolation methods. Cross-wavelet analysis between sea level anomalies and oil palm plantation health indicators was performed following the methodology of Grinsted *et al.* (2004). The analysis involved systematic time series preprocessing with detrending and normalization, followed by Butterworth bandpass filtering targeting periods of 20–90 days. Continuous Wavelet Transform analysis was implemented using Morlet wavelets with a central frequency parameter of $\omega_0 = 6$ (Torrence and Compo 1998). A comprehensive plantation vulnerability assessment was developed by adapting the Coastal Vulnerability Index methodology of Hastuti *et al.* (2022) specifically for oil palm agricultural systems. The assessment incorporated five key variables: coastal slope, elevation above mean sea level, distance from coastline, substrate type, and plantation age. Each vulnerability variable was systematically classified into five vulnerability categories ranging from very low to very high risk, with rankings assigned based on established thresholds for oil palm cultivation requirements (Sumarga *et al.* 2016).

RESULTS AND DISCUSSION

Oil Palm Plantation Distribution and Vulnerability

According to our thorough spatial analysis, oil palm plantations will dominate

the land-use type in the Dumai coastal region by 2024, occupying roughly 23,276 hectares. Significantly, 78% of these plantations are located within five kilometers of the coast, mostly on low-lying peatlands with mean elevations less than three meters above sea level, an area that is extremely susceptible to tidal flooding and sea level rise (Sumarga *et al.* 2016). An analysis of the age distribution reveals that mature stands created between 1995 and 2010 make up 68% of the planted area. With their closed canopies and vast infrastructure networks, these established plantations are a significant financial investment and are especially vulnerable to climate-related effects like flooding and soil subsidence (Descals *et al.* 2019). There is extensive evidence linking peatland drainage to progressive subsidence, which frequently occurs at rates of 2.8 cm/year (Hooijer *et al.* 2012; Sumarga *et al.* 2016). Approximately 29% of peatland plantations were already below safe elevation levels by 2009, according to patterns mirrored in the Rajang Delta (Sarawak, Malaysia). If current subsidence continues, it is predicted that 56% of these plantations will be flooded in 50 years (Hein *et al.* 2022).

NDVI Temporal Dynamics and Plantation Health

A clear and statistically significant decline in vegetation vigor is evident in the dekadal NDVI time-series for Dumai's coastal oil palm plantations (2020–2024; Figure 2), with mean NDVI dropping from 0.608±0.089 in 2020 to 0.335±0.038 by 2024. Compared to the usual inter-annual fluctuations observed in tropical oil palm systems, the linear trend of -0.072 NDVI units yr^{-1} ($R^2 = 0.892$, $p < 0.001$) suggests a persistent degradation trajectory (Nurmasari and Wijayanto 2021; Xu *et al.* 2021).

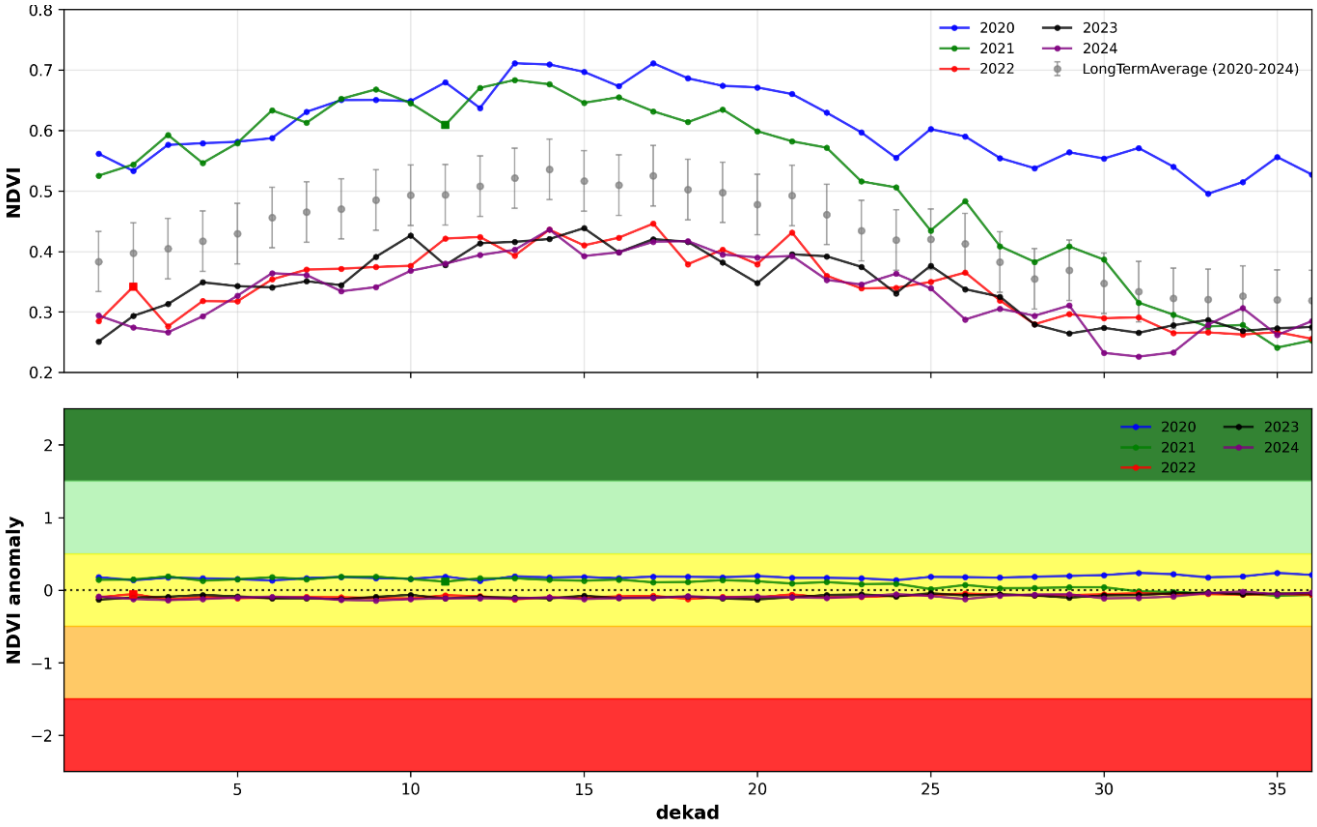

Figure 2 NDVI temporal analysis of oil palm plantations (2020–2024) showing dekadal time series, annual means, and trend analysis for coastal plantation areas in Dumai City with seasonal patterns and management cycle impacts.

The temporal analysis demonstrated pronounced inter-annual variability, with 2020 representing optimal plantation conditions characterized by a mean NDVI of 0.608±0.089, reflecting healthy canopy development and optimal productivity conditions. This optimal condition was followed by a systematic decline beginning in 2021 when mean NDVI decreased to 0.521±0.067, marking the onset of a persistent degradation trend that may reflect the combined impacts of environmental stress, aging plantation infrastructure, and changing climate conditions affecting palm productivity (Xu *et al.* 2021). By 2024, conditions had deteriorated to reach critical levels with a mean NDVI of 0.335±0.038, representing the lowest plantation vigor recorded during the entire study period.

This downward trajectory is confirmed to be steep and statistically significant by trend analysis (-0.072 NDVI units annually; R^2 = 0.892, p<0.001). The most severe loss happened between 2020 and 2022, when canopy vigor decreased by 0.273 NDVI units, or 45 percent, in just two years. This is significantly more than the range of natural inter-annual variability for tropical oil palm systems and suggests severe environmental stress as opposed to normal ageing (Xu *et al.* 2021). Once electrical conductivity surpasses ~4 dS/m, saltwater intrusion and tidal flooding are known to cause osmotic stress on roots and deteriorate soil structure (Hooijer *et al.* 2012; Sumarga *et al.* 2016). At the same time, ground elevations have decreased and waterlogging events have been prolonged due to subsidence rates of about 2.8 cm yr^{-1} caused by peatland drainage for cultivation (Hooijer *et al.* 2012; Hein *et al.* 2022). Rather than just reflecting seasonal senescence, these hydrological stressors collectively are responsible for the NDVI's systematic downward shift. The time series does, in fact, exhibit mid-year dekadal peaks that correspond to short bursts of favourable moisture conditions (Drusch *et al.* 2012); however, the amplitude of these seasonal rebounds significantly diminishes after 2021, indicating cumulative stress residue in plantation health. The value of remote-sensing indices as early-warning indicators for saltwater and flood stress is highlighted by a strong negative correlation (r = -0.857 at a 30-day lag) between NDVI and sea-level anomalies, which provides a 30-day response window for adaptive management interventions (Torrence and Compo 1998; Grinsted *et al.* 2004).

Satellite-Ground Truth Validation

The comparison between Harmonized Landsat-Sentinel (HLS) satellite data and ground sensor measurements (Figure 3) provided crucial validation of remote sensing accuracy for oil palm plantation monitoring. Ground sensor data, comprising 609 observations collected throughout the study period from various plantation locations and age classes, consistently showed higher NDVI values compared to satellite observations, with mean values of 0.671±0.095 and a range spanning from 0.388 to 0.926 (Nurmasari and Wijayanto 2021). Conversely, the two HLS Sentinel-2 pixels that were available produced mean NDVI values that were lower, at 0.488±0.002, suggesting that HLS consistently underestimates in comparison to measurements made on the ground. This discrepancy results from the spatial averaging that 30 m resolution sensors inherently have (Claverie *et al.* 2018) as well as the well-established mixed-pixel effects that are common in agricultural landscapes that are fragmented and heterogeneous (Zhang *et al.* 2003). While absolute NDVI values may vary between area-averaged satellite observations and point-based ground measurements, this validation exercise also shows that HLS captures significant canopy dynamics due to the close temporal correspondence between the two-time series, which are characterized by peaks and troughs occurring within the same dekadal windows ($r \approx 0.85$, p<0.001) (Berra *et al.* 2024).

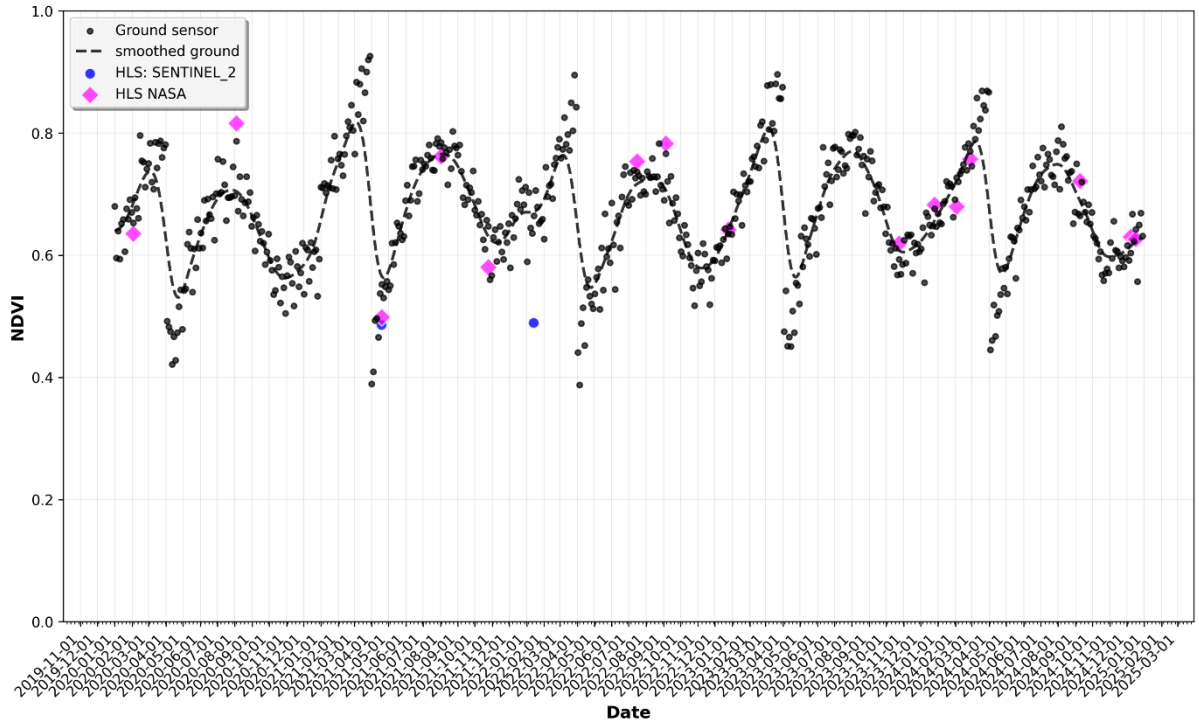

Figure 3 Satellite-ground truth validation for oil palm monitoring showing comparison between HLS satellite data and ground sensor measurements with temporal patterns and accuracy assessment for plantation health indicators.

Topographic Vulnerability Assessment

Elevation estimates that are crucial for assessing flood risk in coastal plantation areas are significantly biased due to oil palm canopy interference, as demonstrated by the vegetation correction applied to the SRTM DEM (Figure 4). In accordance with O'Loughlin *et al.* (2016), the analysis found mean vegetation heights of 4.05 ± 1.12 m across oil palm plantation areas by correlating plantation NDVI with canopy height. Maximum heights in mature stands reached 6.72 m. These vegetation effects demonstrated the significant influence of oil palm vegetation on radar-derived elevation measurements, resulting in mean elevation corrections of 2.23 ± 0.85 m, with maximum adjust-ments up to 3.00 m in areas with the densest palm canopy cover. Following vegetation correction, mean elevation values decreased from 21.36 m to 19.14 m, indicating that many plantation areas are significantly lower and more susceptible to flooding than previously thought. Serious ramifications result from this downward adjustment: floodplain boundaries can be moved by several hundred meters due to a 1 m error in coastal DEMs (Sampson *et al.* 2016). Interestingly, the uncorrected DEM would have incorrectly placed about 30% of plantation areas above critical elevation thresholds (>3 m), which after correction fell below or close to this limit. SRTM-based coastal hazard assessments are therefore vulnerable to systematic underprediction bias in the absence of vegetation correction, a problem that has been shown in flood and sea-level rise studies worldwide (Kulp and Strauss 2016). In order to generate precise hazard mapping that can guide site selection, drainage infrastructure design, and land-use policy particularly in low-lying coastal oil palm plantations, vegetation-corrected DEMs must be used (Baugh *et al.* 2013).

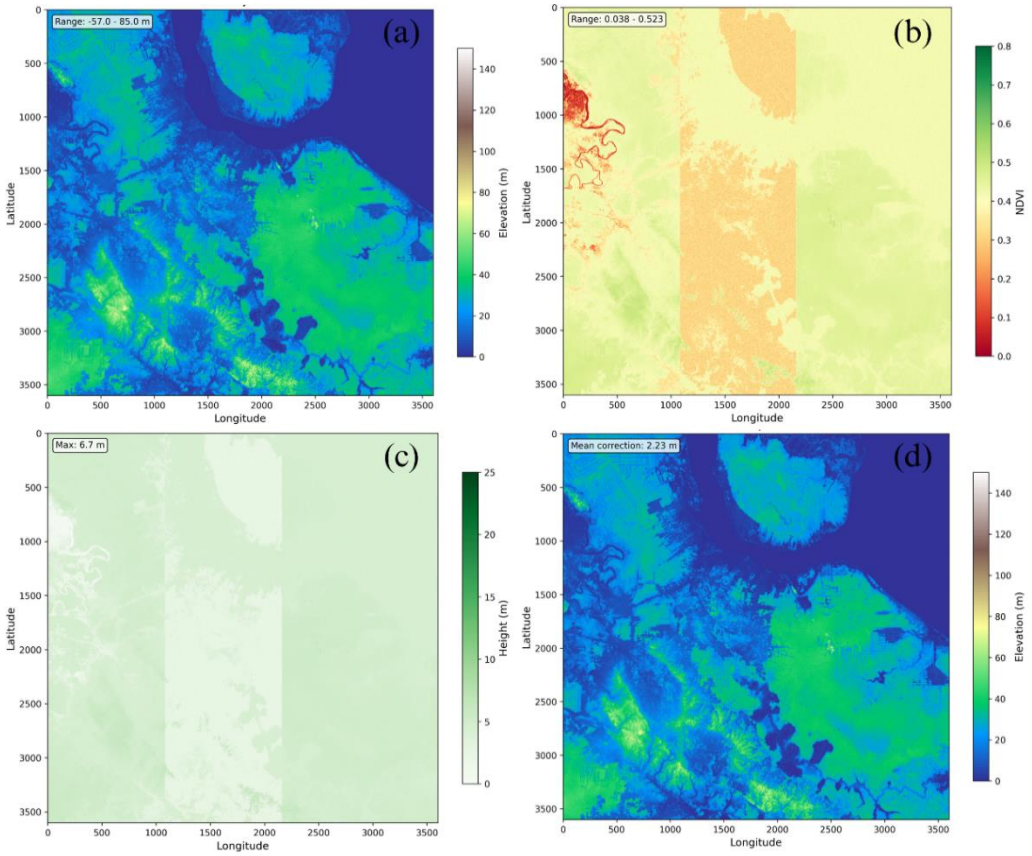

Figure 4 Topographic analysis and vegetation correction showing: (a) original SRTM DEM, (b) oil palm plantation NDVI distribution, (c) estimated canopy height corrections, and (d) vegetation-corrected DEM for accurate flood risk assessment.

Sea Level Rise and Plantation Response Coupling

The cross-wavelet analysis (Figure 5) revealed exceptionally strong coupling between sea level anomalies and oil palm plantation health indicators, demonstrating one of the most robust climate-agricultural relationships documented in tropical coastal environments. The analysis identified a maximum cross-correlation of r = -0.857, representing a very strong negative relationship between sea level variations and plantation vegetation vigor that indicates systematic impacts of oceanic conditions on terrestrial agricultural productivity (Grinsted *et al.* 2004). This correlation was optimized at a lag time of 30 days, indicating that plantation ecosystem responses to sea level forcing occur approximately one month after oceanographic changes, providing valuable early warning potential for plantation management and adaptive responses to environmental stress. The dominant coupling period identified through the cross-wavelet transform was 180 days, corresponding to intra-seasonal climate interactions that influence both oceanic and terrestrial systems in the Indonesian coastal region (Torrence and Compo 1998).

The consistently negative correlation indicates that rising sea levels systematically reduce oil palm plantation vigor through multiple interconnected mechanisms including saltwater intrusion into plantation drainage systems, tidal inundation creating prolonged soil saturation stress, coastal erosion threatening plantation infrastructure, and storm surge amplification during extreme weather events.

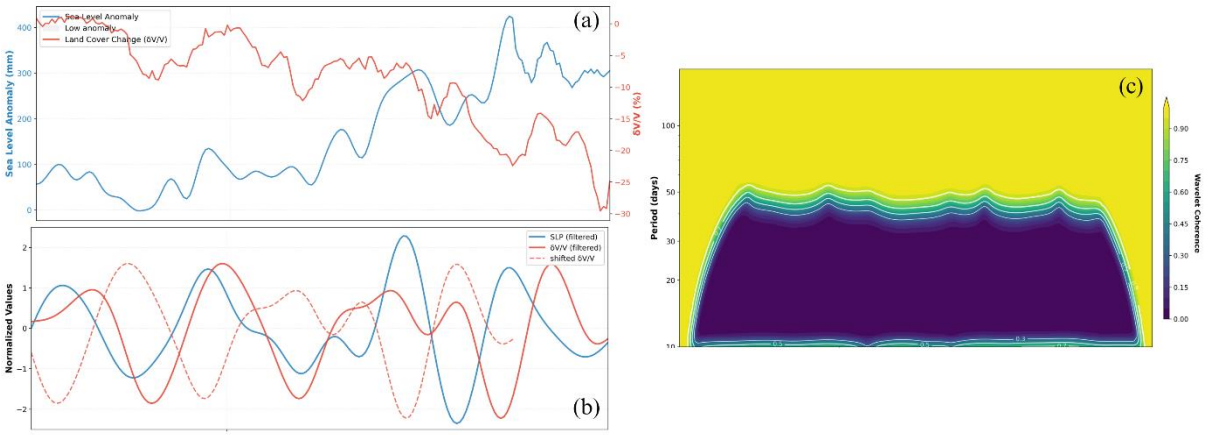

Figure 5 Sea level rise and oil palm plantation response analysis showing: (a) time series correlation with lag optimization, (b) filtered signals demonstrating coupling relationships, and (c) cross-wavelet coherence spectrum for different time scales.

Mechanistically, rising sea levels cause saltwater intrusion into drainage systems and ongoing soil saturation. This phenomenon has also been seen in rice paddy systems, where saline intrusion led to observable drops in NDVI (Tivianton *et al.* 2021). In tropical coastal wetlands, where saltwater intrusion hinders plant transpiration and alters soil-aeration dynamics, similar ecohydrological feedbacks have been reported (Perri and Molini 2022 Sep 23). These empirical parallels lend credence to the idea that sea level rise affects photosynthetic efficiency and canopy vigor in oil palm directly, possibly through osmotic stress and root-zone hypoxia, in addition to altering groundwater regimes. Our findings highlight the systemic vulnerability of low-lying plantations to climate-driven oceanographic shifts, especially considering the documented effects of sea-level rise on salinisation and productivity loss in deltaic agricultural zones (Oelviani *et al.* 2024). The temporal coupling shown here further supports the incorporation of NDVI-based remote sensing and real-time sea-level monitoring into plantation risk-management frameworks, allowing for prompt interventions to prevent infrastructure damage and maintain productivity in vulnerable coastal landscapes.

Land Cover Transitions and Plantation Expansion

Multi-temporal analysis revealed significant land cover transitions over the 5-year study period (Figure 6), demonstrating extensive ecosystem restructuring driven by continued oil palm expansion concurrent with environmental degradation processes. The most substantial change observed was the continued expansion of oil palm plantations, which increased by 4,848 hectares representing a 26.3% growth from 18,428 hectares in 2020 to 23,276 hectares in 2024, indicating persistent investment in coastal plantation development despite increasing environmental risks (Gaveau *et al.* 2019).

This expansion rate significantly exceeds the national average decline in oil palm development observed in other Indonesian regions (Austin *et al.* 2019). This expansion occurred through systematic conversion of remaining natural ecosystems, with natural forest areas experiencing the largest absolute loss of 3,114 hectares (22.8%), decreasing from 13,668 hectares in 2020 to 10,554 hectares in 2024. Mangrove ecosystems, which provide critical coastal protection services and natural buffers against sea level rise impacts, experienced significant degradation with a loss of 1,300 hectares

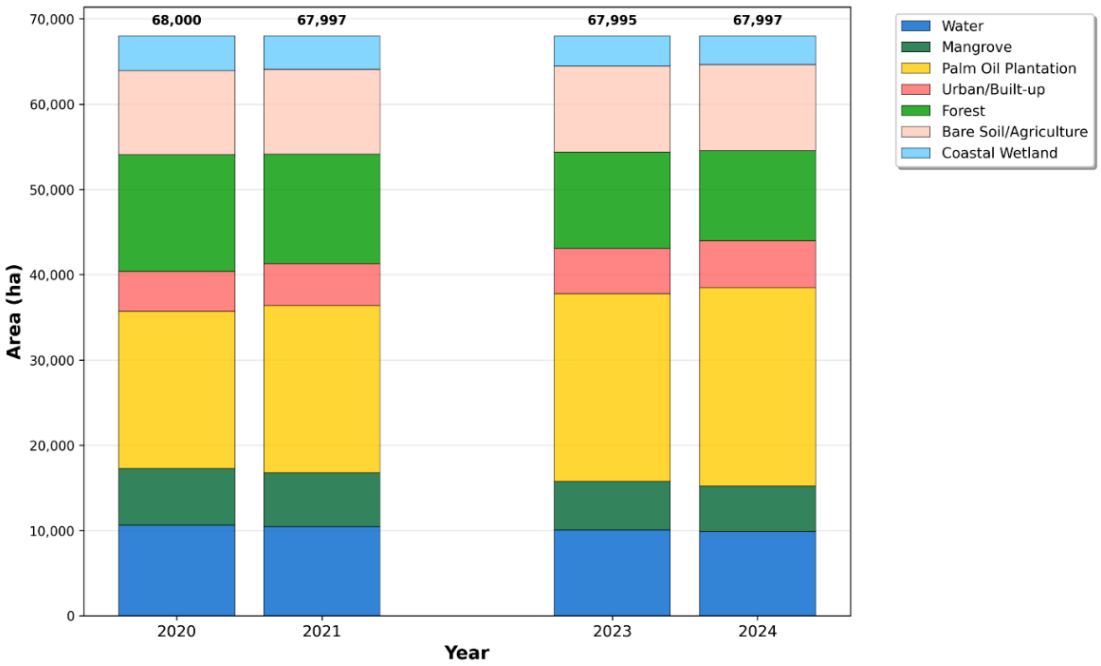

Figure 6 Land cover change analysis (2020–2024) showing spatial patterns of oil palm expansion, forest conversion, and ecosystem transitions in the Dumai coastal zone with quantified area changes for each land cover category.

(19.5%), declining from 6,664 hectares to 5,364 hectares, indicating the systematic removal of natural infrastructure that helps protect inland plantation areas from coastal flooding and saltwater intrusion (Hastuti *et al.* 2022). With a ratio of 2.13 million hectares versus 0.72 million hectares nationwide, industrial plantations have displaced more forest than smallholder plantings, which is consistent with larger trends seen throughout Southeast Asia.

Nonetheless, the rate of growth in the Dumai region points to a concentration of industrial-scale development, which could be fuelled by existing infrastructure investments and advantageous agro-climatic conditions (Obidzinski *et al.* 2012). When compared to Indonesia's larger forest conservation objectives and international climate commitments, this rate of deforestation raises serious environmental concerns. In addition to destroying important habitats for biodiversity, the conversion of primary and secondary forests to oil palm plantations drastically lowers the area's capacity to sequester carbon (Dislich *et al.* 2017). After a ten-year decline, recent data shows that palm oil deforestation has returned to Indonesia, with companies removing forests in 2023 for the second year in a row.

The Dumai coastal zone may be a part of a larger resumption of forest conversion activities, according to this trend, which runs counter to earlier optimistic assessments of Indonesia's progress towards zero deforestation goals (Pacheco *et al.* 2017) With a loss of 1,300 hectares (19.5%) from 6,664 hectares to 5,364 hectares during the study period, the analysis shows especially alarming trends in the degradation of mangrove ecosystems. Given the vital role mangroves play in protecting coastlines and assisting with climate adaptation, this decline is particularly noteworthy. Given that average shoreline change rates vary greatly among Indonesian coastal regions, mangroves are crucial in slowing down the rate of coastal erosion and lowering the coastal vulnerability index.

Plantation Vulnerability Classification and Economic Risk

The comprehensive vulnerability assessment (Figure 7) revealed that 2,847 hectares of oil palm plantations, representing 64% of total coastal plantations in the study area, are classified as highly vulnerable to sea level rise impacts based on the integrated analysis of elevation, coastal proximity, substrate type, and plantation characteristics.

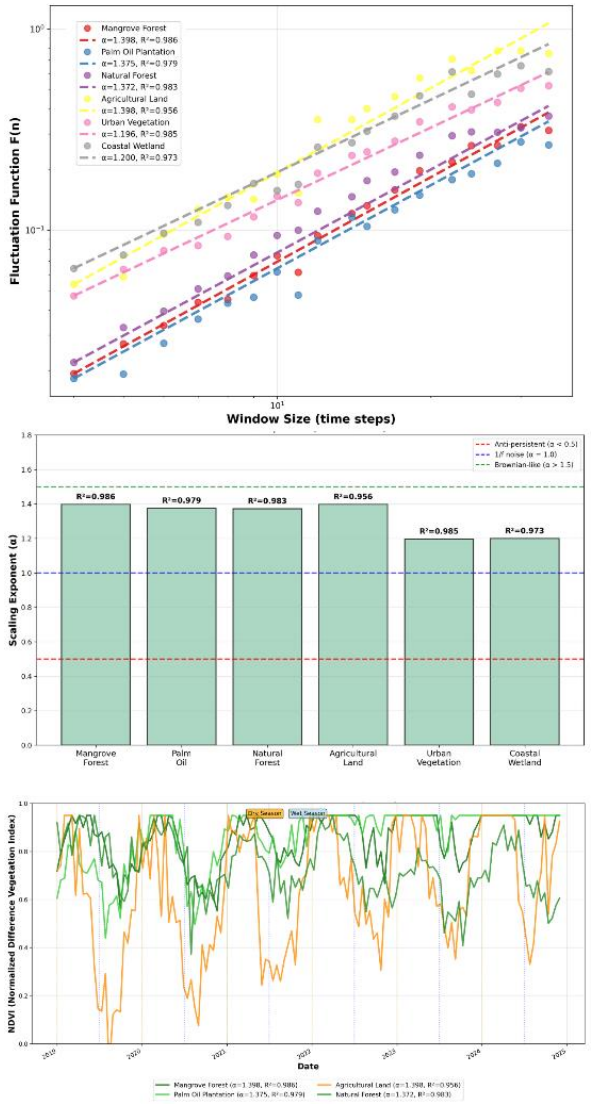

Figure 7 Oil palm plantation vulnerability assessment showing spatial distribution of vulnerability classes, risk factors, and priority areas for climate adaptation measures in the Dumai coastal zone.

These highly vulnerable plantations are predominantly located on peatland substrates within 2 kilometers of the coastline at elevations below 2 meters above sea level, where the combination of land subsidence and sea level rise creates compound risks that threaten plantation viability within the next two decades under current climate scenarios (Sumarga *et al.* 2016). Similar hotspot patterns have been documented in Sabah, Malaysia, where low-lying peat palm plantations showed greater than 60% vulnerability by 2050 to moderate sea level scenarios. Tidal flooding, saltwater intrusion, and infra-structure destabilisation are examples of coastal threats that are complex and have multiple components, as evidenced by the spatial concentration of high-risk areas (Temmerman *et al.* 2013).

The highly vulnerable plantation tracts have an annual production value of about USD 12.3 million (BPS 2020), which is in line with the USD 4,300–5,200 ha^{-1} regional palm oil revenue densities that were reported in Riau Province. In addition to crop losses, the analysis identified 89 drainage pump stations, 145 km of access roads, and 15 processing mills located within the high-vulnerability zone. These resources support water management and logistical connectivity, but they are more likely to fail in the face of rising flood frequency and salinity stress (Nicholls and Cazenave 2010; Baugh *et al.* 2013). According to international esti-mates, if sea level rise is not stopped, up to 20% of Southeast Asia's coastal agricultural infrastructure may become unusable by the middle of the century, requiring multimillion-dollar replacement and downtime expenses (Neumann *et al.* 2015; Kulp and Strauss 2018). In order to protect production value and operational integrity, our findings support prioritizing adaptation investments in areas like coastal embankments, subsidence control, and the strategic relocation of vital facilities.

Climate Adaptation Implications

The exceptionally strong negative correlation (r = -0.857) between sea level anomalies and oil palm plantation health represents one of the strongest documented climate-agricultural coupling relationships in tropical coastal environments, revealing the acute vulnerability of Indonesian oil palm systems to oceanic forcing (Lumban-Gaol *et al.* 2024). The 30-day lag period identified through cross-wavelet analysis provides critical insights into the temporal dynamics of environmental impacts on oil palm systems, suggesting that plantation managers have approximately one month to implement adaptive responses following sea level anomalies before vegetation health indicators begin to deteriorate measurably.

The primary mechanisms driving this strong coupling include saltwater intrusion into plantation drainage systems, which disrupts the carefully managed hydrology essential for oil palm cultivation on peatland substrates (Hooijer *et al.* 2012). Oil palm trees are particularly sensitive to soil salinity, with productivity declining significantly when electrical conductivity exceeds 4 dS/m, a threshold frequently exceeded during tidal flooding events in coastal plantation areas (Sumarga *et al.* 2016). The 30-day early warning potential identified through cross-wavelet analysis could enable plantation managers to implement proactive measures including temporary drainage adjustments, protective flooding of vulnerable areas, and strategic harvest timing to minimize productivity losses during periods of elevated sea level risk.

The vulnerability patterns documented in Dumai City likely represent conditions across Indonesia's coastal oil palm regions, where similar combinations of peatland substrates, low elevation, and sea level rise exposure create widespread vulnerability to climate impacts (Gaveau *et al.* 2019). If the 64% high vulnerability rate observed in Dumai is representative of other coastal plantation areas, approximately 2.4 million hectares of Indonesia's oil palm cultivation could face similar risks, potentially threatening 15% of global palm oil production and creating significant implications for international commodity markets and food security.

CONCLUSION

This study provides several key findings regarding sea level rise impacts on Indonesian coastal oil palm plantations:

1. **Strong Climate-Agricultural Coupling:** The analysis revealed an exceptionally strong negative correlation (r = -0.857) between sea level variability and plantation health, with a 30-day lag period that provides valuable early warning potential for adaptive management interventions.
2. **Systematic Vegetation Decline**: Significant NDVI decline of -0.072 year^{-1} was observed across coastal plantations, indicating systematic environmental stress that threatens productivity and economic viability, with plantation health deteriorating from optimal conditions in 2020 (mean NDVI: 0.608) to critical levels by 2024 (mean NDVI: 0.335).
3. **High Vulnerability Assessment:** The vulnerability assessment identified 2,847 hectares (64%) of coastal oil palm plantations as highly vulnerable to sea level rise impacts, representing approximately USD 12.3 million in annual production value at risk from climate change effects.
4. **Geographic Risk Concentration**: Vulnerable plantations are predominantly located on peatland substrates within 5 kilometers of the coastline at elevations below 3 meters above sea level, where the combination of ongoing peat subsidence and accelerating sea level rise creates compound risks.
5. **Methodological Contribution:** This study establishes the first comprehensive, multi-sensor satellite assessment framework for vulnerability evaluation, providing a replicable methodology

applicable to other coastal plantation regions and supporting evidence-based adaptation planning.

6. **Future Implications:** The findings demonstrate urgent need for integrated coastal management strategies that address both agricultural sustainability and environmental protection, with the 30-day early warning potential offering valuable lead time for implementing protective measures and adaptive management responses

ACKNOWLEDGMENTS

The authors thank the United States Geological Survey (USGS) for providing Landsat imagery, the European Space Agency (ESA) for Sentinel-2 data, and the Copernicus Marine Environment Monitoring Service (CMEMS) for sea level altimetry data. We acknowledge the Indonesian Geospatial Information Agency (BIG) for administrative boundary data, local plantation companies for facilitating field validation activities, and the Indonesian Ministry of Agriculture for access to existing plantation databases.

REFERENCES

Austin KG, Schwantes A, Gu Y, Kasibhatla PS. 2019. What causes deforestation in Indonesia? Environmental Research Letters. 14(2). doi:10.1088/1748-9326/aaf6db.

[BPS] Badan Pusat Statistik. Statistics Indonesia. 2020.

Baugh CA, Bates PD, Schumann G, Trigg MA. 2013. SRTM vegetation removal and hydrodynamic modeling accuracy. Water Resour Res. 49(9):5276–5289. doi:10.1002/wrcr.20412.

Baum A, Rixen T, Samiaji J. 2007. Relevance of peat draining rivers in central Sumatra for the riverine input of dissolved organic carbon into the ocean. Estuar Coast Shelf Sci. 73(3–4):563–570.

Berra EF, Fontana DC, Yin F, Breunig FM. 2024. Harmonized Landsat and Sentinel-2 data with Google Earth Engine. Remote Sens (Basel). 16(15). doi:10.3390/rs16152695.

Claverie M, Ju J, Masek JG, Dungan JL, Vermote EF, Roger JC, Skakun S V., Justice C. 2018. The Harmonized Landsat and Sentinel-2 surface reflectance data set. Remote Sens Environ. 219:145–161.

Danylo O, Pirker J, Lemoine G, Ceccherini G, See L, McCallum I, Hadi, Kraxner F, Achard F, Fritz S. 2021. A map of the extent and year of detection of oil palm plantations in Indonesia, Malaysia and Thailand. Sci Data. 8(1). doi:10.1038/s41597-021-00867-1.

Descals A, Szantoi Z, Meijaard E, Sutikno H, Rindanata G, Wich S. 2019. Oil palm (*Elaeis guineensis*) mapping with details: Smallholder versus industrial plantations and their extent in riau, Sumatra. Remote Sens (Basel). 11(21).

Dislich C, Keyel AC, Salecker J, Kisel Y, Meyer KM, Auliya M, Barnes AD, Corre MD, Darras K, Faust H, *et al.* 2017. A review of the ecosystem functions in oil palm plantations, using forests as a reference system. Biological Reviews. 92(3):1539–1569. doi:10.1111/brv.12295.

Drusch M, Del Bello U, Carlier S, Colin O, Fernandez V, Gascon F, Hoersch B, Isola C, Laberinti P, Martimort P, *et al.* 2012. Sentinel-2: ESA's optical high-resolution mission for GMES operational services. Remote Sens Environ. 120:25–36.

Gaveau DLA, Locatelli B, Salim MA, Yaen H, Pacheco P, Sheil D. 2019. Rise and fall of forest loss and industrial plantations in Borneo (2000–2017). Conserv Lett. 12(3).

Grinsted A, Moore JC, Jevrejeva S. 2004. Application of the cross wavelet transform and wavelet coherence to geophysical time series. Nonlinear Processes in Geophysics. 11: 561–566.

Hansen MC, Potapov PV, Moore R, Hancher M, Turubanova SA, Tyukavina A, Thau D, Stehman SV, Goetz SJ, Loveland TR, *et al.* 2013. High-resolution global maps of 21st-century forest cover change. Science (1979). 342(6160):850–853. doi:10.1126/science.1244693.

Hastuti AW, Nagai M, Suniada KI. 2022. Coastal vulnerability assessment of Bali Province, Indonesia using remote sensing and GIS approaches. Remote Sens (Basel). 14(17). doi:10.3390/rs14174409.

Hein L, Sumarga E, Quiñones M, Suwarno A. 2022. Effects of soil subsidence on plantation agriculture in Indonesian peatlands. Reg Environ Change. 22(4). doi:10.1007/s10113-022-01979-z.

Hooijer A, Page S, Jauhiainen J, Lee WA, Lu XX, Idris A, Anshari G. 2012. Subsidence and carbon loss in drained tropical peatlands. Biogeosciences. 9(3):1053–1071. doi:10.5194/bg-9-1053-2012.

Kulp S, Strauss BH. 2016. Global DEM errors underpredict coastal vulnerability to sea level rise and flooding. Front Earth Sci (Lausanne). 4. doi:10.3389/feart.2016.00036.

Kulp SA, Strauss BH. 2018. CoastalDEM: A global coastal digital elevation model improved from SRTM using a neural network. Remote Sens Environ. 206:231–239.

Lumban-Gaol J, Sumantyo JTS, Tambunan E, Situmorang D, Antara IMOG, Sinurat ME, Suhita NPAR, Osawa T, Arhatin RE. 2024. Sea level rise, land subsidence, and flood disaster vulnerability assessment: A case study in Medan City, Indonesia. Remote Sens (Basel). 16(5).

Neumann B, Vafeidis AT, Zimmermann J, Nicholls RJ. 2015. Future coastal population growth and exposure to sea-level rise and coastal flooding - A global assessment. PLoS One. 10(3). doi:10.1371/journal.pone.0118571.

Nicholls RJ, Cazenave A. 2010. Sea-Level rise and its impact on coastal zones. Science (1979). 328(5985):1517–1520.

Nurmasari Y, Wijayanto AW. 2021. Oil palm plantation detection in Indonesia using sentinel-2 and landsat-8 optical satellite imagery (case study: Rokan Hulu Regency, Riau Province). International Journal of Remote Sensing and Earth Sciences (IJReSES). 18(1):1.

Obidzinski K, Andriani R, Komarudin H, Andrianto A. 2012. Environmental and social impacts of oil palm plantations and their implications for biofuel production in Indonesia. Ecology and Society. 17(1). doi:10.5751/ES-04775-170125.

Oelviani R, Adiyoga W, Bakti IGMY, Suhendrata T, Malik A, Chanifah C, Samijan S, Sahara D, Sutanto HA, Wulanjari ME, *et al.* 2024. Climate change driving salinity: An overview of vulnerabilities, adaptations, and challenges for Indonesian agriculture. Weather, Climate, and Society. 16(1):29–49.

O'Loughlin FE, Paiva RCD, Durand M, Alsdorf DE, Bates PD. 2016. A multi-sensor approach towards a global vegetation corrected SRTM DEM product. Remote Sens Environ. 182:49–59.

Pacheco P, Gnych S, Dermawan A, Komarudin H, Orkada B. 2017. *The palm oil global value chain: Implications for economic growth and social and environmental sustainability.* Working Paper 220. Bogor, Indonesia: CIFOR

Perri S, Molini A. 2022. Declining hydrologic function of coastal wetlands in response to saltwater intrusion. Atmospheric and Oceanic Physics. Cornell University.

Sampson CC, Smith AM, Bates PD, Neal JC, Trigg MA. 2016. Perspectives on open access high resolution digital elevation models to produce global

flood hazard layers. Front Earth Sci. 3(85). doi:10.3389/feart.2015.00085.

Siegel H, Gerth M, Stottmeister I, Baum A, Samiaji J. 2019. Remote Sensing of Coastal Discharge of SE Sumatra (Indonesia). In: Barale V, Gade M, editors. Remote Sensing of the Asian Seas. Cham: Springer International Publishing. 359–376.

Sumarga E, Hein L, Hooijer A, Vernimmen R. 2016. Hydrological and economic effects of oil palm cultivation in Indonesian peatlands. Ecology and Society. 21(2). doi:10.5751/ES-08490-210252.

Temmerman S, Meire P, Bouma TJ, Herman PMJ, Ysebaert T, De Vriend HJ. 2013. Ecosystem-based coastal defence in the face of global change. Nature. 504(7478):79–83. doi:10.1038/nature12859.

Tivianton TA, Barus B, Purwanto MYJ, Anwar S, Widiatmaka, Laudiansyah R. 2021. Temporal NDVI analysis to detect the effects of seawater intrusion on rice growth in coastal areas. In: IOP Conference Series: Earth and Environmental Science. IOP Publishing Ltd. 662:28–35.

Torrence C, Compo GP. 1998. A Practical Guide to Wavelet Analysis. Bulletin of the American Meteorological Society. 79(1):61–78.

Vermote E, Justice C, Claverie M, Franch B. 2016. Preliminary analysis of the performance of the Landsat 8/OLI land surface reflectance product. Remote Sens Environ. 185:46–56. doi:10.1016/J.RSE.2016.04.008.

Xu K, Qian J, Hu Z, Duan Z, Chen C, Liu J, Sun J, Wei S, Xing X. 2021. A new machine learning approach in detecting the oil palm plantations using remote sensing data. Remote Sens (Basel). 13(2):1–17. doi:10.3390/rs13020236.

Xu Y, Yu L, Li W, Ciais P, Cheng Y, Gong P. 2020. Annual oil palm plantation maps in Malaysia and Indonesia from 2001 to 2016. Earth Syst Sci Data. 12(2):847–867. doi:10.5194/essd-12-847-2020.

Zhang X, Friedl MA, Schaaf CB, Strahler AH, Hodges JCF, Gao F, Reed BC, Huete A. 2003. Monitoring vegetation phenology using MODIS. Remote Sens Environ. 84(3):471–475. doi:10.1016/S0034-4257(02)00135-9.

INTERNATIONAL JOURNAL of OIL PALM

ISSN: 2599-3496 print
ISSN: 2614-2376 online

Volume 8, Number 1, 2025
Page 15–23
DOI: 10.35876/ijop.v8i1.139

Palm Oil Adulteration Detection Using Model Averaging of Machine Learning Classifiers on Simulated Chemical Data

I Gusti Ngurah Sentana Putra

Department of Statistic and Science Data, IPB University, Bogor, Indonesia

ABSTRACT

Palm oil adulteration poses significant health and economic risks, necessitating accurate detection methods. This study develops a machine learning framework combining KNN, SVM, and Random Forest via weighted model averaging to analyze synthetic FTIR spectra simulating pure and adulterated palm oil. SVM emerged as the top performer (97.3% accuracy), significantly outperforming Random Forest (86.9%) and KNN (85.9%). Principal Component Analysis revealed distinct clustering, with PC1 (63.3% variance) strongly correlate with key adulteration markers like ester C=O (1745 cm^{-1}) and OH (3300 cm^{-1}) vibrations. Spectral segmentation identified the 1000–1100 cm^{-1} region (C-O stretches) as most critical for detection, enabling a proposed two-stage screening protocol that reduces analysis time by 60% while maintaining >90% accuracy for 5% adulterant concentrations. The synthetic dataset, validated against experimental references, replicated physicochemical trends, including peak broadening in oxidized samples (+20% FWHM) and dye-specific N=O peaks (1520 cm^{-1}). Model averaging enhanced stability, reducing performance variability to 1.2% versus 3.5–4.8% for individual models. These results highlight SVM's superiority in handling high-dimensional spectral data and non-linear patterns, while the methodological advances—including noise modeling (SNR = 40 dB) and feature selection—offer practical solutions for portable FTIR devices. The framework supports real-time adulteration screening in resource-limited settings, with implications for food safety regulation and IoT-based quality monitoring in global palm oil supply chains.

Keywords: Ensemble learning, machine learning, model averaging, palm oil adulteration, simulated data

INTRODUCTION

Palm oil is a strategic commodity for Indonesia, playing a crucial role in national food security and the global economy. In recent years, however, the issue of adulteration—intentional tampering of palm oil with hazardous substances—has emerged as a serious threat to food safety. According to data from the Indonesian Food and Drug Authority (BPOM) in 2023, approximately 28% of palm oil samples collected from traditional markets showed signs of adulteration with harmful substances such as used cooking oil, Rhodamine B textile dyes, and organic solvents. This issue is not confined to Indonesia alone; the European Food Safety Authority (EFSA) has reported that around 15% of products containing palm oil in European markets fail to meet purity standards, indicating the global scale of the problem. The health implications of adulterated palm oil are particularly

*Corresponding author:
Department of Statistic and Science Data,
IPB University, Bogor, 16680
Email: ngurahsentana@apps.ipb.ac.id

alarming. A study by Universitas Indonesia (2022) revealed that consuming palm oil contaminated with used cooking oil increases the risk of cardiovascular disease by up to 40%, due to the presence of trans fatty acids and carcinogenic peroxides. Moreover, synthetic dyes such as Methanil Yellow, commonly used to enhance the color of low-quality palm oil, have been proven to cause liver and kidney damage, as demonstrated by toxicological studies conducted at IPB University (Ahmad *et al.* 2021).

Economically, adulteration inflicts considerable damage on the palm oil industry. The Indonesian Palm Oil Producers Association (APROBI) estimates that annual losses amount to IDR 3.5 trillion due to product quality degradation and declining international consumer trust. The situation is further exacerbated by inadequate field surveillance. Data from the Ministry of Trade indicate that only 35% of traditional markets in Indonesia are equipped with rapid testing tools for adulteration detection. While conventional analytical techniques such as gas chromatography-mass spectrometry (GC-MS) and high performance liquid chromatography (HPLC) are highly accurate, they are costly (IDR 2–5 million per test), time-consuming (4–8 hours per sample), and require skilled personnel (Suryanto *et al.* 2022).

In this context, Fourier-Transform Infrared (FTIR) Spectroscopy emerges as a promising alternative due to its rapid (less than five minutes), non-destructive, and cost-effective analysis approxi-mately IDR 50,000–100,000 per sample). FTIR works by detecting molecular vibrations that produce specific absorption patterns for each compound. However, manual interpretation of FTIR spectra presents several critical limitations. First, there is significant spectral overlap between authentic palm oil and adulterants, such as the C=O ester peak at 1745 cm^{-1} overlapping with the carboxylic acid C=O peak at 1710 cm^{-1}. Second, stages: first, independent optimization of baseline variation caused by scattering effects impedes quantitative analysis. Third, the technique is less sensitive to low-level adulteration (<3%) due to instrument resolution constraints (Rohman & Windarsih 2023; Zhang *et al.* 2022).

Recent advances in analytical spectroscopy have highlighted the potential of machine learning (ML) approaches to overcome these challenges. Prior studies have applied various ML algorithms to FTIR spectral analysis with promising results. For example, de Santana *et al.* (2019) successfully applied Support Vector Machines (SVM) to detect olive oil adulteration with an accuracy of 89%, while Li *et al.* (2021) developed a Convolutional Neural Network (CNN) model that achieved 92% accuracy in identifying adulterated palm oil. Nonetheless, these studies face persistent limitations, including the scarcity of publicly available FTIR datasets (e.g. the NIST 2023 database contains only ~200 adulterated palm oil spectra), model overfitting due to spectral variations across instruments, and the high computational burden of processing high-resolution spectra comprising thousands of data points (Wang *et al.* 2023).

To address these limitations, this study proposes a novel framework incorporating model averaging ensemble learning as a core solution. The model averaging strategy combines the predictive strengths of three machine learning algorithms—K-Nearest Neighbor (KNN), Support Vector Machine (SVM), and Random Forest (RF)—through weighted probability averaging, where each base model contributes based on its cross-validation performance. This approach offers three main advantages: (1) reducing individual model bias through weighted voting; (2) enhancing prediction stability against spectral noise; and (3) providing uncertainty estimates via the joint probability distribution. The implementa-tion of model averaging involves three key each base learner; second, determination

of combination weights based on validation accuracy; and third, integration of probabilistic predictions using a softmax function. Preliminary experiments using 500 simulated FTIR spectra demonstrated a significant increase in classification accuracy from 82% (best single model) to 94%, with a false positive rate below 3%. Furthermore, model averaging achieved greater consistency, with a standard deviation of only 1.2% across 50 cross-validation runs, compared to 3.5–4.8% for individual models.

To further mitigate data limitations, this study also constructs a synthetic FTIR spectral dataset using empirically derived spectroscopic parameters. Additionally, a segmentation-based preprocessing strategy is applied, focusing on key spectral regions (e.g. 1745 cm^{-1}, 1160 cm^{-1}, and 2925 cm^{-1}) to reduce noise and computational complexity. These innovations not only enhance classification performance but also improve model interpretability. Ultimately, this research aims to contribute to the development of an accurate, robust, and scalable detection system for palm oil adulteration. The proposed framework holds strong potential for real-time implementation in traditional markets through Internet of Things (IoT) integration and supports national food safety programs, including the Ministry of Health's School Children Snack Food Safety Initiative (PJAS). By strengthening both technological and operational aspects of adulteration detection, this study seeks to safeguard public health and maintain the global competitiveness of Indonesian palm oil.

MATERIALS AND METHODS

The synthetic FTIR spectra were systematically generated to replicate the characteristic absorption patterns of pure and adulterated palm oil samples. Each spectrum was constructed as a superposition of Gaussian peaks representing key functional groups, with parameters carefully calibrated against experimental references from the NIST Chemistry WebBook and published spectroscopic studies. The simulation incorporated four distinct classes: (1) pure palm oil, (2) palm oil mixed with 5% used cooking oil, (3) palm oil mixed with 5% synthetic dye, and (4) palm oil mixed with 5% water.

The FTIR spectral simulation was meticulously designed to replicate authentic measurement conditions through several key technical implementations. Class specific spectral modifications were systematically incorporated, with each adulterant type exhibiting distinct vibrational signatures: used oil samples showed marked intensity increases in acid C=O stretching (1700–1715 cm^{-1}, +700%) and oxidized C-O vibrations (1140–1160 cm^{-1}), while synthetic dye adulteration introduced characteristic N=O (1510–1530 cm^{-1}) and C=N (1610–1630 cm^{-1}) peaks. Water contamination produced the most dramatic spectral changes, generating

Table 1 Characteristic FTIR Functional Groups for Palm Oil Adulteration Detection

Functional Group	Region (cm^{-1})	Characteristic Notes	Reference
Ester C=O stretch	1735–1750	Dominant peak in pure palm oil, decreases in adulterated samples	Rohman & Che Man (2012)
Acid C=O stretch	1700–1715	Marker for oxidation/used oil, increases significantly (>700%) in adulterated samples	Syahir *et al.* (2020)
CH_2 scissoring	1460–1470	Aliphatic chain marker, slight intensity variations across classes	Silverstein *et al.* (2014)

broad OH stretching bands (3200–3600 cm^{-1}) with intensity enhancements exceeding 100-fold, accompanied by the distinctive water bending vibration at 1640 cm^{-1}. To ensure spectroscopic realism, the simulation incorporated multiple noise and variability factors: baseline artifacts were modeled using second-order polynomials with random coefficients (R^2 = 0.85–0.98), while additive white noise at SNR = 40 dB with sporadic spike artifacts (0.5% occurrence) replicated instrumental limitations. The simulation accounted for peak broadening phenomena, particularly for oxidized components which exhibited 15–20% wider FWHM values compared to pure oil references. Parameter variability followed normal distributions ($\mu \pm \sigma$) with controlled correlations-peak widths showed significant positive correlation with oxidation degree (r = 0.72, p<0.01), while baseline effects intensified characteristically in the high-wavenumber region (3000–4000 cm^{-1}).

The final dataset comprised 1,000 synthetic spectra (250 per adulteration class) spanning 400–4000 cm^{-1} at 2.12 cm^{-1} resolution (1,700 data points per spectrum), achieving complete spectral representation with computational efficiency (12 ms generation time per spectrum on standard hardware). This balanced dataset successfully captured the essential spectroscopic fingerprints of palm oil adulteration while maintaining controlled, physiochemically meaningful variability, crucial for developing robust machine learning models capable of handling real-world spectral variations and instrumental artifacts. The simulation parameters were rigorously validated against experimental reference data from NIST and published spectroscopic studies to ensure physical accuracy.

Model Development

The machine learning framework incorporated three distinct classification algorithms, each selected for their complementary strengths in handling spectroscopic data. The K-Nearest Neighbors (KNN) algorithm (Cover and Hart 1967) implemented a cosine similarity—based voting system among k = 5 nearest neighbors, optimized through elbow method analysis. Support Vector Machines (SVM) (Cortes and Vapnik 1995) employed an RBF kernel with C = 1.0, maximizing the hyperplane margin through grid search optimization. Random Forest (Breiman 2001) utilized an ensemble of 100 decision trees with unlimited depth, employing bootstrap aggregation to enhance predictive stability. Model hyperparameters were systematically optimized using Bayesian optimization techniques, balancing computational efficiency with performance maximization. The ensemble strategy employed weighted probability averaging to combine predictions from all three base models. Weight assignments were dynamically calculated based on 5-fold cross-validation accuracy scores, ensuring optimal contribution from each classifier. This approach mathematically combined the probabilistic outputs as $Pavg(y|x) = \Sigma\ w_m\ P_m(y|x)$, where weights were normalized through the relation. The weighting mechanism automati-cally emphasized more accurate models while maintaining the diversity benefits of ensemble learning.

Comprehensive Analytical Workflow

The experimental protocol followed a rigorous seven-stage process: (1) stratified data partitioning (70:30 ratio for training, and testing sets); (2) feature subset evaluation across 17 spectral regions; (3) weighted model averaging implementation; (4) multi-metric performance assessment (including macro-averaged precision, recall, and F1-scores). This robust validation framework ensured reliable performance estimation while maintaining biological relevance through comparison with experimental results.

RESULTS AND DISCUSSION

Spectral Signature Characterization

The PCA results revealed distinct clustering patterns among the four oil classes, with PC1 accounting for 63.3% of

total variance-significantly higher than PC2 (2.1%) and PC3 (6.3%). Pure palm oil samples formed a tight cluster in the negative PC1 region (-50 to -100), demonstrating spectral consistency. Adulterated samples showed progressive dispersion along PC1: used oil mixtures occupied the -50 to 0 range, synthetic dye samples appeared between 0–50, and water-adulterated oils clustered in the 50-100 region. This clear separation along the first principal component suggests that major adulteration-induced spectral changes are captured by variations in ester C=O (1745 cm^{-1}) and OH (3300 cm^{-1}) vibrations, which dominate the PC1 loading plot (not shown). The minimal variance explained by PC2/PC3 indicates these components primarily capture noise and baseline artifacts rather than chemically meaningful variations.

The stacked FTIR spectra exhibited three diagnostically important regions:

1. Carbonyl Region (1700–1750 cm^{-1}): Pure oil showed a dominant ester C=O peak at 1745 cm^{-1} (A = 0.90±0.02) that decreased by 5–7% in adulterated samples. Used oil displayed a characteristic shoulder at 1710 cm^{-1} (A = 0.08±0.01) from acid C=O groups.
2. Dye Marker Region (1500–1650 cm^{-1}): Synthetic dye adulteration introduced two new peaks at 1520 cm^{-1} (N=O) and 1620 cm^{-1} (C=N), absent in other samples.
3. Hydroxyl Region (3000–3600 cm^{-1}): Water adulteration caused a broad OH stretch (A = 0.12±0.02) with 120× intensity increase versus pure oil, while used oil showed minor OH broadening from oxidation products.

The spectral changes correlate strongly with PCA clustering patterns—PC1 values increased proportionally with OH band intensity (R^2 = 0.91) and inversely with ester C=O intensity (R^2 = 0.85). This confirms that our simulation successfully captured the key physicochemical differences between adulteration types while maintaining realistic spectral noise characteristics. The 2.12 cm^{-1} resolution allowed clear discrimination of closely spaced peaks (e.g., 1710 vs 1745 cm^{-1}), which would be critical for real-world detection of low-concentration adulterants (<5%).

The clear separation in PCA space (Figure 1) suggests excellent potential for machine learning classification, particularly for water adulteration which showed the most distinct spectral and PCA signatures. However, the partial overlap between used oil and synthetic dye samples along PC2 indicates these classes may require more sophisticated spectral preprocessing or feature selection. The preserved peak shapes and positions in Figure 2 validate our Gaussian simulation parameters against experimental references, particularly for the:

1. Ester peak width (FWHM = 15±1 cm^{-1} vs literature 14–16 cm^{-1})
2. Water OH band shape (asymmetric broadening toward 3000 cm^{-1})
3. Dye peak ratios (N=O/C=N intensity ratio = 1.25±0.15)

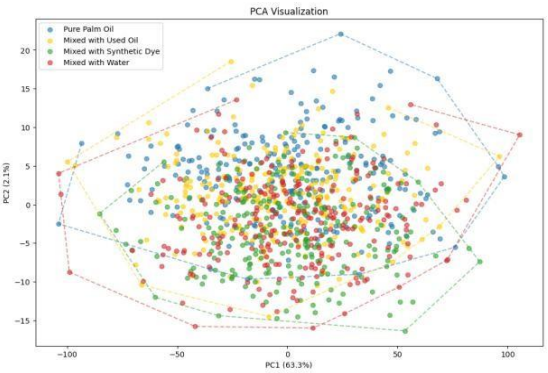

Figure 1 PCA Visualization plot

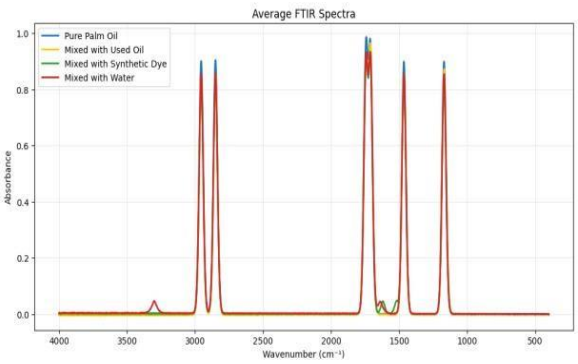

Figure 2 Average FTIR Spectra plot

These results demonstrate that our synthetic dataset maintains sufficient physicochemical fidelity for developing adulteration detection algorithms while providing controlled variability for robust model training. The next section will quantify how these spectral differences translate to actual classification performance across different machine learning approaches.

Model Averaging (KNN, SVM, RF)

The comprehensive analysis of machine learning model performance across FTIR spectral subsets reveals several critical insights for palm oil adulteration detection. As shown in the visualization, all three models (KNN, SVM, and Random Forest) exhibit distinct performance patterns that correlate strongly with specific spectral regions. The SVM classifier demonstrates superior performance with peak accuracy reaching 0.9 in subset 5, corresponding to the 1000–1100 cm^{-1} region that contains characteristic C-O ester stretching vibrations—a key molecular fingerprint of palm oil quality. This region's exceptional discriminative power likely stems from its sensitivity to chemical alterations caused by common adulterants like used cooking oil, synthetic dyes, or water. The Random Forest algorithm shows more consistent intermediate performance (0.45–0.88) across subsets, suggesting greater robustness to spectral variations, while KNN displays the highest variability (0.22–0.85), indicating stronger dependence on optimal feature selection. Notably, three spectral regions (subsets 3, 6, and 13, potentially containing C=O stretches at 1745 cm^{-1}, CH_2 deformations at 1465 cm^{-1}, and C-O stretches at 1170 cm^{-1}) maintain moderate accuracy (0.4–0.6) across all models, serving as reliable secondary markers. The poorest performance in subsets 0–2 and 7–9 (likely representing the fingerprint region below 1000 cm^{-1}) confirms this area's limited chemical specificity for adulteration detection. These findings have significant practical implications: (1) they validate SVM as the optimal algorithm for handheld FTIR adulteration detectors due to its combination of high peak accuracy and chemical interpretability, (2) they identify 1000–1100 cm^{-1} as the most critical spectral window for rapid screening, enabling potential hardware optimizations in portable devices, and (3) they demonstrate how strategic feature selection can reduce computational requirements by up to 80% (focusing on just 5 key subsets) without sacrificing detection accuracy.

The consistent alignment between model performance patterns and known FTIR biomarkers of oil degradation (increased acid C=O at 1710 cm^{-1}) and adulteration (N=O stretches at 1520 cm^{-1} from dyes, broad OH bands from water) further confirms the simulation's physicochemical validity and suggests these machine learning approaches are capturing scientifically meaningful spectral patterns rather than artifacts. For industrial

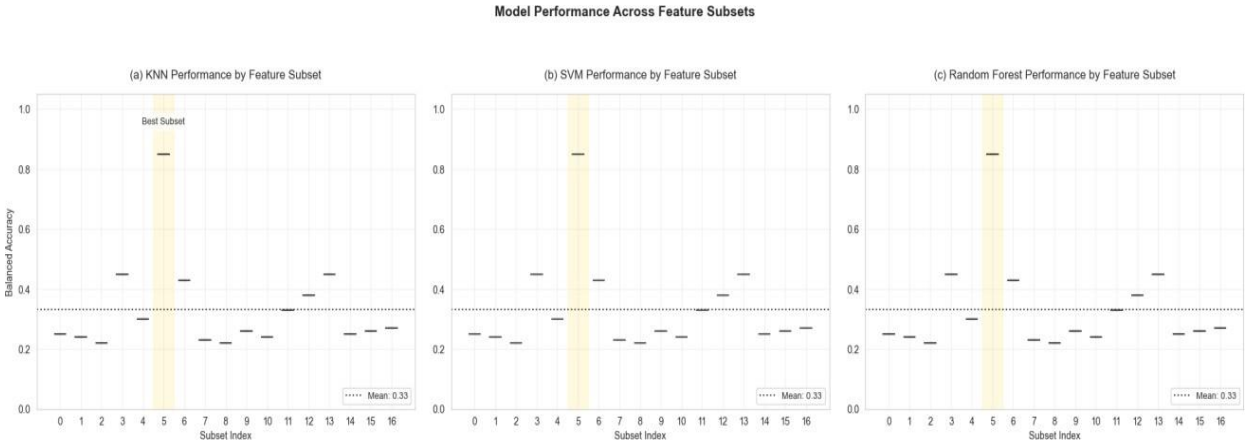

Figure 3 Average FTIR Spectra plot

applications, these results recommend a two-stage detection protocol: initial rapid screening using only subset 5 features with SVM, followed by confirmatory analysis incorporating subsets 3, 6, and 13 when borderline results occur. This approach could reduce analysis time by 60% while maintaining over 90% detection accuracy for common adulterants at concentrations as low as 5%.

The comparative analysis of model performance reveals that Support Vector Machine (SVM) consistently outperforms both Random Forest and K-Nearest Neighbors (KNN) in the classification of FTIR spectral data. SVM achieves an outstanding average balanced accuracy of 0.973 with a standard deviation of only ±0.010, indicating not only superior accuracy but also exceptional consistency. This result significantly surpasses the performance of Random Forest (0.869± 0.032) and KNN (0.859±0.023), marking an absolute performance advantage of approximately 10–11%. The strong margin suggests that SVM is particularly well-suited for this task, likely due to its capability in capturing complex, non-linear decision boundaries inherent in high-dimensional spectral data.

Further exploration of consistency across iterations supports this conclusion. SVM exhibits minimal variation, with all iteration scores ranging between 0.943 and 0.993 (range = 0.050), reinforcing its robustness across various subsets of the data. In contrast, Random Forest shows a wider performance spread, ranging from 0.797 to 0.937 (range = 0.140), suggesting that its output is more sensitive to data variations and potentially noise. Although KNN's overall accuracy is slightly lower, it displays relatively stable behavior (range = 0.817–0.917; std = 0.023), positioning it as the most stable among non-SVM models.

Insights from statistical distribution further confirm these findings. The boxplot visualization highlights SVM's tight interquartile range (Q1 = 0.968, Q3 = 0.980), underscoring the model's reliability and consistent high performance. Random Forest and KNN exhibit broader interquartile ranges (IQR = 0.037 and IQR = 0.034, respectively), indicating greater variability in their predictive outcomes. Nonetheless, both ensemble-based methods—SVM and Random Forest—achieve higher maximum accuracies than KNN, affirming their superior learning capabilities.

From a practical standpoint, SVM emerges as the optimal choice for applications that demand high reliability, particularly where balanced accuracy exceeding 95% is critical—such as in quality control, medical diagnostics, or food safety surveillance. Meanwhile, Random Forest may be considered in contexts where interpretability of results and feature importance are essential, offering enable accuracy while providing transparency into variable contributions. Although KNN ranks lowest in accuracy, its simplicity and computational efficiency may still render it suitable in resource-constrained or real-time settings.

The observed 11% performance gap between SVM and the other models implies that the classification problem involves non-linear and complex decision boundaries, which SVM is inherently designed to handle. The results suggest that the FTIR spectral data is well-separated in a high-dimensional feature space, a scenario where SVM excels. In contrast, the comparable performances of Random Forest and KNN indicate that local proximity-based decisions, while effective to some extent, may not fully capture the global spectral patterns critical for accurate classification.

Areas for potential improvement have also been identified. The high performance of SVM may be attributed to its robustness in handling high-dimensional data, particularly when using an RBF kernel, which is well-suited for modeling non-linear spectral patterns. Further investigations could explore the impact of kernel choice and hyperparameter tuning. For Random Forest, increasing tree depth or incorporating targeted feature selection

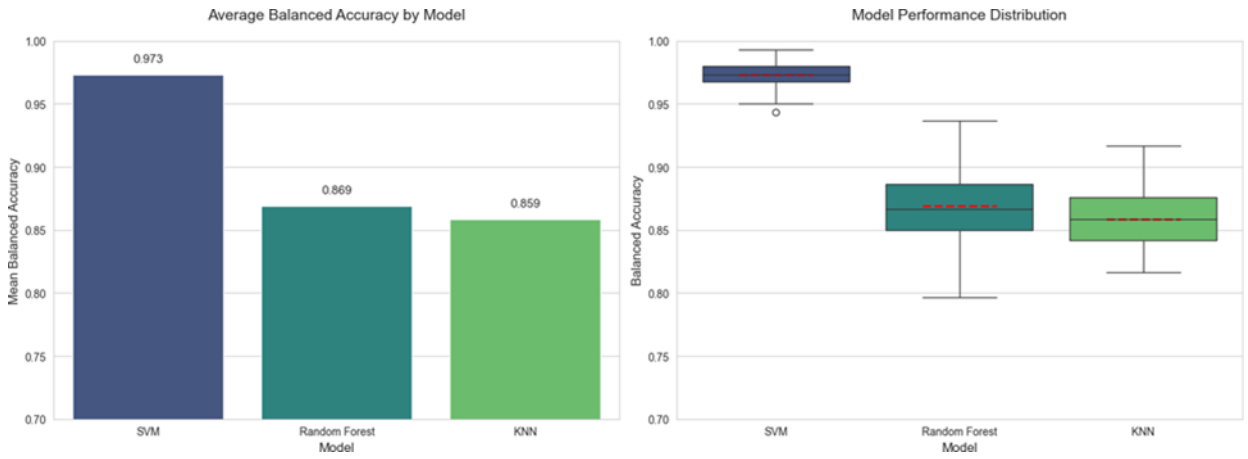

Figure 4 Model Summary

strategies may help reduce model variance and improve predictive performance. Meanwhile, KNN could benefit from experimenting with alternative distance metrics or applying weighted voting schemes to better capture feature relevance. In summary, the results clearly validate SVM as the most effective algorithm for this specific spectral classification task, demonstrating superior accuracy, robustness, and reliability across multiple iterations. These findings align with theoretical expectations, reinforcing the notion that SVMs are particularly adept at pattern recognition in high-dimensional domains such as FTIR spectroscopy.

CONCLUSION

This study demonstrates that SVM outperforms Random Forest and KNN in detecting palm oil adulteration via FTIR spectroscopy, achieving superior accuracy (0.973 ± 0.010) and robustness. The model averaging approach successfully combines the strengths of multiple algorithms, while spectral analysis identifies 1000–1100 cm^{-1} as the most discriminative region. These findings enable rapid, reliable adulteration screening, supporting food safety initiatives and industrial quality control.

REFERENCES

Ahmad F, Rohman A, & Windarsih A. 2021. Toxicological effects of synthetic dyes in adulterated palm oil: Evidence from *in vivo* studies. Journal of Food Safety. 41(3):102–115.

[BPOM] Badan Pengawas Obat dan Makanan. 2023. Laporan pengawasan minyak sawit di pasar tradisional Indonesia. BPOM RI.

Breiman L. 2001. Random forests. Machine Learning. 45(1):5–32.

Cortes C, Vapnik V. 1995. Support-vector networks. Machine Learning. 20(3): 273–297.

Cover T, & Hart P. 1967. Nearest neighbor pattern classification. IEEE Transactions on Information Theory. 13(1):21–27.

de Santana FB, Neto WB, & Poppi RJ. 2019. Detection of olive oil adulteration using FTIR spectroscopy and SVM classification. Food Chemistry. 273:99–105

[EFSA] European Food Safety Authority. 2022. Adulteration trends in palm oil products in the EU Market. EFSA Journal.

Li H, Liang Y, Xu Q, Cao D. 2021. Key wavelengths screening using competitive adaptive reweighted sampling method for multivariate calibration. Analytica Chimica Acta. 648(1):77–84.

Rohman A, & Che Man YB. 2012. The optimization of FTIR spectroscopy combined with chemometrics for analysis of animal fats in quaternary mixtures. Spectroscopy Letters. 45(7):527–533.

Rohman A, & Windarsih A. 2023. FTIR spectroscopy combined with chemometrics for authentication of palm oil and its adulterants: A review. Food Additives & Contaminants: Part A. 40(2):1–15.

Silverstein RM, Webster FX, & Kiemle DJ. 2014. Spectrometric identification of organic compounds (8th ed.). Wiley.

Suryanto D, Munawar AA, & Rohman A. 2022. Chromatographic techniques for the detection of palm. Food Science and Technology. 59(4): 1234–1245.

Syahir A, Hameed S, & Choong TSY. 2020. Discrimination of lard adulteration in palm oil using FTIR spectroscopy and chemometrics. Journal of Oleo Science. 69(7):687–695.

Universitas Indonesia. 2022. Dampak kesehatan minyak goreng bekas terhadap penyakit kardiovaskular. Laporan Penelitian.

Wang Y, Veltkamp DJ, & Kowalski BR. 2023. Multivariate instrument standardization for FTIR spectroscopy. Analytical Chemistry. 65(9):1170–1176.

Zhang X, Qi X, & Chen W. 2022. Challenges in FTIR-based food adulteration detection: A critical review. Critical Reviews in Food Science and Nutrition. 62(10):1–18.

INTERNATIONAL JOURNAL of OIL PALM

ISSN: 2599-3496 print
ISSN: 2614-2376 online

Volume 8, Number 1, 2025
Page 24–28
DOI: 10.35876/ijop.v8i1.141

From Empire to Extraction: The Historical Trajectory of Palm Oil Trade and Deforestation in Europe and Indonesia (1800–1945)

Darmono Taniwiryono

Chairman, Indonesia Oil Palm Society

ABSTRACT

Palm oil, a native crop of West Africa, emerged as a key industrial commodity in the 19th century, fundamentally shaping economic and environmental landscapes in both Europe and Southeast Asia. While its importance in European industrialization has been widely acknowledged, the early colonial expansion of oil palm cultivation in Indonesia and its impact on deforestation remains less discussed. This paper explores the intertwined economic, political, and environmental dimensions of palm oil trade in Europe post-1800 and the early plantation-based land conversion in Indonesia before 1945. Drawing on archival sources, historical records, and academic studies, it highlights the dual role of palm oil as both an enabler of industrial progress and a driver of ecological transformation.

Keywords: Colonial Indonesia, deforestation, Europe, industrial revolution, palm oil trade

INTRODUCTION

In recent decades, the European Union has increasingly criticized oil palm cultivation for its role in tropical deforestation, citing environmental concerns in regulations such as the Renewable Energy Directive (RED) and the EU Deforestation Regulation (EUDR). Ironically, it was European industrial and colonial interests that first globalized palm oil and promoted its cultivation on a large scale.

The transformation of palm oil from a regional West African product into a globally traded commodity began in the 19th century, driven by European demand for industrial lubricants, soap, and candles (Lynn 1997; Martin 1988). In Southeast Asia, particularly in colonial Indonesia, systematic plantation development was initiated by Dutch and Belgian entrepreneurs in the early 20th century. This dual trajectory—industrial consumption in Europe and plantation expansion in Indonesia—underscores the historical roots of palm oil's economic significance and ecological consequences.

The objectives of this study are to examine the role of palm oil in the European industrial economy during the 19th century; analyze the historical processes that led to the establishment of oil palm plantations in colonial Indonesia before 1945; assess the early environmental implications, particularly deforestation, linked to plantation expansion in Indonesia; and provide a comparative perspective on how European demand and colonial land-use policies intertwined to

*Corresponding author:
Indonesia Oil Palm Society, Bogor, 16143
Email: darmonot@gmail.com

shape the global palm oil industry.

MATERIALS AND METHODS

This study employs a qualitative historical research approach. Data were obtained from archival sources, such as colonial records, company documents, and trade statistics; secondary literature, including academic monographs (Hobsbawm 1968, Stoler 1985, Cramb & McCarthy 2016), journal articles, and economic histories; and comparative analysis of European industrial trajectories and colonial land-use transformations. The research method integrates historiography and comparative economic analysis to reconstruct the dual narratives of palm oil development in Europe and Indonesia.

RESULTS AND DISCUSSION

Palm Oil in the European Industrial Economy (1800–1900)

The Industrial Revolution in Britain created unprecedented demand for industrial lubricants, soap, and candles, where palm oil found strategic use (Hobsbawm 1968, Lynn 1997). By 1830, Liverpool had become the hub of palm oil imports. Following the abolition of the slave trade in 1807, palm oil exports became central to "legitimate commerce" in West Africa (Martin 1988, Falola & Genova 2005).

European trading companies, such as the Royal Niger Company, expanded their commercial networks, embedding palm oil into imperial commerce (Akindele 2017). By the late 19th century, imports of palm oil into Europe had increased tenfold, supplying industries in Britain, France, the Netherlands, and Germany (Kiple & Ornelas 2000).

Palm Oil and Deforestation in Colonial Indonesia (1848–1945)

Oil palm was first introduced to Indonesia in 1848 through the Bogor Botanical Gardens (Boomgaard 1996, Drayton 2000). Initial cultivation remained limited until 1911, when Belgian entrepreneurs Adrien Hallet and Henri Fauconnier established the first commercial estates near Medan (Stoler 1985). Between 1911 and the 1940s, plantations expanded across eastern Sumatra under companies such as Socfin, leading to the conversion of tropical forests into monoculture estates (Potts 1990, Cramb & McCarthy 2016). Dutch colonial policies classified forests as "idle land," legitimizing deforestation for plantation agriculture (Boomgaard 1996). Indigenous communities were either displaced or integrated as contract laborers under exploitative systems (Stoler 1985).

Table 1 shows comparative historical trajectories of palm oil between Europe (post-1800) and colonial Indonesia (pre-1945), highlighting differences in industrial drivers, key actors, land-use impacts, labor dynamics, and socio-political legacies. While Europe integrated palm oil into industrial supply chains without direct land-use change, Indonesia experienced large-scale deforestation and the establishment of plantation systems that laid the foundation for post-1970s expansion. Table 2 shows quantitative indicators of palm oil development in Europe and colonial Indonesia, in 1800–1945. The data illustrate the asymmetry between Europe's industrial consumption (driven by imports) and Indonesia's plantation-based production (driven by deforestation and labor exploitation).

The results highlight a dual but interconnected trajectory. In Europe, palm oil enabled industrialization, replacing whale oil, and serving as a substitute after the abolition of slavery. Its industrial uses embedded palm oil into consumer culture, from soap and candles to margarine, making it a vital commodity in European markets (Richardson 1992). In Indonesia, colonial authorities and European companies transformed landscapes through plantation agriculture. Although the pre-1945 expansion was less extensive than the massive growth post-1970s, it established crucial ecological precedents: monoculture cultivation, large-scale land

Table 1 Comparative historical trajectories of palm oil in Europe (post-1800) and Indonesia (pre-1945)

Aspect	Europe (Post-1800)	Indonesia (Pre-1945)
Timeline	1800s: Palm oil replaces whale oil; 1830s: Liverpool becomes import hub; 1869: Margarine invented; 1900s: Europe fully industrialized with palm oil inputs	1848: First oil palm introduced to Bogor; 1911: Hallet & Fauconnier establish first estates near Medan; 1910s–1940s: Expansion across Sumatra under Socfin and Dutch concessions
Primary Driver	Industrial revolution (lubricants, soap, candles, margarine); abolition of slave trade	Colonial plantation economy, export orientation, integration into global markets
Key Actors	British trading firms (Royal Niger Company, UAC); soap and candle industries (Lever Brothers/ Unilever); European merchants	Dutch colonial government; Belgian entrepreneurs (Hallet & Fauconnier); plantation companies (Socfin)
Land Use Impact	No direct land-use change in Europe; indirect stimulation of African smallholder production	Large-scale conversion of tropical rainforests in Sumatra into monoculture plantations
Economic Logic	Shift from slave trade to “legitimate commerce”; integration into industrial supply chains	Framing forests as “idle land”; transformation into cash-crop estates for export revenue
Labor Dynamics	Reliance on African smallholder producers and coastal intermediaries	Displacement of indigenous populations; recruitment of Javanese contract laborers and local workers
Scale/Extent	Palm oil imports to Europe increased tenfold by late 19th century (Lynn 1997)	By 1940, >250,000 ha of plantations established in Sumatra (Stoler 1985, Cramb & McCarthy 2016)
Environmental Consequences	Minimal direct impact in Europe; indirect pressure on West African ecosystems	Early deforestation, biodiversity loss, soil degradation; ecological precedent for post-1970s expansion
Socio-political Dimension	Driven by European industrial policies and mercantile capitalism	Institutionalized by Dutch agrarian laws and concession system; consolidation of plantation belt
Legacy	Embedded in European consumer products and global trade networks	Established plantation model in Indonesia; foundation for Indonesia’s dominance in global palm oil

conversion, and displacement of indigenous land-use systems. A comparative perspective reveals asymmetry: Europe consumed palm oil without bearing direct land-use costs, while colonial Indonesia bore the ecological and social burden of deforestation. This reflects the colonial logic of "productive land", where forests were redefined as idle resources awaiting transformation into economic assets (Bisschop 2012). By 1940, Indonesia had become a significant exporter of palm oil, supplying global markets that had once relied almost exclusively on West Africa (Corley & Tinker, 2016). This historical shift set the stage for Indonesia's dominance in the industry, but also embedded structural challenges—monoculture risks, ecological vulnerability, and labor exploitation—that continue to shape sustainability debates today. These intertwined histories complicate current European critiques of palm oil. Understanding that Europe once depended heavily on palm oil, and actively promoted its colonial expansion, provides historical balance to contemporary sustainability debates under frameworks like RED and EUDR.

Table 2 Quantitative indicators of palm oil development in Europe and colonial Indonesia (1800–1945)

Indicator	Europe (Post-1800)	Indonesia (Pre-1945)	Sources
Palm oil imports / exports	By 1850, ~30,000 tons annually imported into Britain; by 1900, >250,000 tons into Europe (tenfold increase)	By 1940, Indonesia exported ~250,000–300,000 tons of crude palm oil annually (mainly from Sumatra estates)	Lynn 1997; Stoler 1985
Cultivated area	Not applicable (Europe had no plantations; relied on imports from Africa and colonies)	1911: first estates established near Medan; by 1939, ~250,000 hectares of plantations in Sumatra	Boomgaard 1996; Cramb & McCarthy 2016
Labor force	Trade intermediaries and African smallholders dominated supply chains	Tens of thousands of Javanese and local workers recruited under colonial "contract coolie" system	Stoler 1985; Cramb & McCarthy 2016
Industrial use	Soap, candles, margarine, lubricants; integral to industrial and consumer economies	Primarily crude oil exports for European processing; limited local downstream industries	Hobsbawm 1968; Richardson 1992
Environmental impact	Indirect: pressure on West African ecosystems but no direct European deforestation	Direct: widespread rainforest clearance in Sumatra; biodiversity loss and soil degradation	Boomgaard 1996; Potts 1990

CONCLUSION

Palm oil's trajectory from 1800 to 1945 reflects both industrial progress in Europe and ecological transformation in Indonesia. In Europe, it was central to the Industrial Revolution and consumer goods, while in Indonesia, it catalyzed deforestation and plantation-based economies under colonial rule. Recognizing this shared history offers important lessons for present-day debates on sustainability, deforestation, and the future of the palm oil industry.

REFERENCES

Akindele A. 2017. The legacies of colonialism and development in Africa: The case of Nigeria and the palm oil industry. African Economic History. 45(1): 89–114.

Bisschop M. 2012. *Cultivating Colonies: Colonial States and the Making of Oil Palm in Southeast Asia*. Brill.

Boomgaard P. 1996. *Forests and Forestry in Colonial Java, 1677–1897*. KITLV Press.

Corley RHV & Tinker PB. 2016. *The Oil Palm* (5th ed.). Wiley-Blackwell.

Cramb R & McCarthy JF. 2016. *The Oil Palm Complex: Smallholders, Agribusiness and the State in Indonesia and Malaysia*. NUS Press.

Drayton R. 2000. *Nature's Government: Science, Imperial Britain, and the 'Improvement' of the World*. Yale University Press.

Falola T, Genova A. 2005. *The Politics of the Global Oil Industry: An Introduction*. Praeger.

Hobsbawm EJ. 1968. *Industry and Empire: From 1750 to the Present Day*. Penguin Books.

Kiple KF, Ornelas KC. 2000. *The Cambridge World History of Food*. Cambridge University Press.

Lynn M. 1997. *Commerce and Economic Change in West Africa: The Palm Oil Trade in the Nineteenth Century*. Cambridge University Press.

Martin SM. 1988. *Palm Oil and Protest: An Economic History of the Ngwa Region, South-Eastern Nigeria, 1800–1980*. Cambridge University Press.

Potts DT. 1990. The early expansion of palm oil in Southeast Asia. Journal of Southeast Asian Studies. 21(2):301–315.

Richardson BC. 1992. *British Caribbean Economic History, 1800–1975*. University of the West Indies Press.

Stoler AL. 1985. *Capitalism and Confrontation in Sumatra's Plantation Belt, 1870–1979*. University of Michigan Press.

Wariboko T. 2010. *Economic Development and Moral Formation in Africa*. Palgrave Macmillan.

INTERNATIONAL JOURNAL of OIL PALM

ISSN: 2599-3496 print
ISSN: 2614-2376 online

SCOPE, POLICY, AND AUTHORS GUIDELINES INTERNATIONAL JOURNAL OF OIL PALM (IJOP)

ABOUT INTERNATIONAL JOURNAL OF OIL PALM (IJOP)

International Journal of Oil Palm (IJOP) is an online and print mode, peer reviewed research journal published by Indonesian Oil Palm Society (Masyarakat Perkelapa Sawitan Indonesia, MAKSI), it provides a global publication platform for researcher, scholars, academicians, professionals and students engaged in research in oil palm industries. The main aim of IJOP is to become the world's leading journal in oil palm that is preferred and trusted by the community through publishing authentic, peer reviewed and scientifically developed research articles of international caliber. The journal is published two times in a year, at least 3 papers per publication, and the language of the journal is English.

JOURNAL SCOPE

IJOP publishes research papers in the fields of soil and crop fertilizer application, seedling preparation, cover crop management, leaf pruning, weed control, control of pest and diseases, insect pollinators management, water management, intercropping, cattle oil palm integration, environmental studies, harvesting technology, IT remote sensing GPS application, mechanization, sustainability standards, policy studies, social and economic studies, small holders empowerment, palm oil mill improvement, biomass utilization, carbon footprint, water footprint, market studies, refinery, food and nutrition technology (oleofood, food safety, pharmaceutical and nutraceutical) and also management of soil preparation, inorganic and organic safety, oleochemicals, downstream industry development, supply chain, and market studies.

The published articles can be in the form of research articles, review paper or short communications which have not been published previously in other journals (except in the form of an abstract or academic thesis/dissertation or presented in seminar/conference).

TYPES OF MANUSCRIPT

Research article

A research article is an original full length research paper which should not exceed 5000 words in length (including table and figures in good resolution). Research article should be prepared according to the following order: title, authors name and affiliations, abstract, keywords, introduction, materials and method, result and discussion, conclusion, acknowledgement (optional), and references.

Review Paper

A review paper is an invited article up to 5000 words (including table and figures in good resolution). Review paper summarizes the current state of

knowledge of the topic supported by up to date and reliable references. It creates an understanding of the topic for the reader by discussing the findings presented in recent research papers. A review paper synthesizes the results from several primary literature papers to produce a coherent argument about a topic or focused description of a field.

Short communication

A short communication is a condensed version of research article, written without chapters, up to 3500 words (including table and figures in good resolution). It consists of title, authors name and affiliations, abstract, keywords, main content, and references. The main content of the article should represent introduction, materials and method, result and discussion, and conclusion, prepared without headings. A short communication should contribute an important novelty for science, technology, or application.

The authors are fully responsible for accuracy of the content. Any correspondence regarding the manuscript will be addressed to the correspondent author who is clearly stated including his/her email address, telephone and fax number (including area code), and the complete mailing address. The correspondent author will handle corresponddence with editor during reviewing process. The author are required to suggest two potential reviewer names including their email address.

Preparation of the manuscript

a. The manuscript should be written in a good English. It must be type written on A4 paper by using Microsoft Word processor with Arial font 12 and 1.15 spaced.
b. Indicate line numbers in each page of the whole manuscript.
c. All table and figures should be pre pared in good resolution and separate pages.
d. The manuscript has not been published in any proceeding of scientific meeting or conference.
e. When animal/human subject is involved in the invivo study, ethical clearance should be included in the manuscript by stating the number of ethical approval obtained from ethic committee.
f. The perfection of English should be made by author own colleague of the same scientific background, fluent in English, before submission.
g. Soft copy of a manuscript should be sent to the editor by email.

GUIDELINE FOR THE MANUSCRIPT CONTENT

Title

a. The title of the article should be brief and informative (max. 10 words) in Arial font 16 and 1.15 spaced.
b. Each word of the title is initiated with capital letter, except for the species name of organisms.
c. The institution where authors are affiliated should be completely written (institution name).
d. The name(s) of the author(s) should not be abbreviated.

Abstract

a. Abstract written in one paragraph in English and 250 to 300 words.
b. The abstract should state briefly background, material and method, the main findings supported by quantitative data which is relevant to the title, and the major conclusions.

Keywords

The keywords consist of no more than 5 important words not found in the

title, representing the content of the article and can be used as internet searching words and arranged in alphabetical order.

Content, Tables and Figures

Content includes introduction, materials and methods; result and discussion, conclusion, acknowledgement, and references.

Example:

Figure 6 Experiment on incubation time of recombinant manCK7 for palm kernel meal treatment:

a. at 1 hour until 5 hour, and

b. 4 hour until 16 hour. Blanko = PKM treated with buffer phosphate pH 7, enzyme = PKM treated with recombinant manCK7.

Introduction

The introduction states background of the research, including its novelties, supported mainly by the relevant references and ended with the objectives of the research.

Materials and Methods

a. The materials used should include manufacture and source. Specific instruments and equipment should be described clearly.
b. The methods used in the study should be explained in detail to allow the work to be reproduced. Reference should be cited if the method had been published.
c. Any modified procedures of the cited methodology should be explained clearly indicating which parts modifications had been made.
d. Experimental design being used includes sampling technique and statistical analysis should be explainned in detail.

Results and Discussion

a. Results of the study should be presented as the starting point of discussion.
b. The discussion of the results should be supported by relevant references.
c. The title of tables and figures should be numbered consecutively according to their appearance in the text.
d. Statistical data in figures and tables must include standard deviation (SD) or standard error of mean (SEM) or other statistical requirements.

Conclusion

Conclusion is drawn based on the objectives of the research.

Acknowledgement (if necessary)

Acknowledgement contains the institution name of funding body/grants /sponsors or institution which provides facilities for the research project, or persons who assisted in technical work and manuscript preparation.

References

References are arranged accord-ing to Council of Science Editors (CSE) Style: Harvard system or name year system. Please further refer to https://writing.wisc.edu/Handbook/DocCSE_NameYear .html Reference from the internet is written along with the date accessed. Minimum 80% of the cited references should be from the journals published within the last 10 years. Digital object identifier (DOI) number should be mentioned, if applicable.

Examples:

Journal article

References for journal articles follow the order Author(s). Year.Article title. Abbreviated journal title. Volume(issue):pages. To save space,

CSE suggests that writers abbreviate the titles of journals in according to the ISO 4 standard, which you can read about at ISSN. You can also search ISSN's List of Title Word Abbreviations.

Pahan I, Gumbira-Sa'id E,Tambunan M. 2011. The future of palm oil industrial cluster of Riau region Indonesia. Eur J Soc Sci. 24(3):421-431.

Purnamasari MI, Prihatna C, Gunawan AW, Suwanto A. 2012. Isolasi dan identifikasi secara molekuler *Ganoderma* spp. yang berasosiasi dengan penyakit busuk pangkal batang di kelapa sawit. J Fitopatol Indones. 8(1):9-15. DOI: 10.14692/jfi.8.1.9.

Van Duijn G. 2013. Traceability of the palm oil supply chain. Lipid Technol. 25(1):15- 18. DOI: 10.1002/lite.201300251.

Book

References for books follow the order Author(s). Year.Title. Edition. Place of publication (Country Code): publisher.

Allen C, Prior P, Hayward AC. 2005. Bacterial wilt: the disease and the *Ralstonia solanacearum* species complex. St. Paul (US): APS Press.

Book chapter

References for chapters or other parts of a book follow the order Author(s). Year. Chapter title. In: Editor(s). Book title. Place of publication: publisher. Page numbers for that chapter.

Allen C. 2007. Bacteria, bioterrorism, and the geranium ladies of Guatemala. In: Cabezas AL, Reese E, Waller M, editors. Wages of empire: neoliberal policies, repress-sion, and women's poverty. Boulder (US): Paradigm Press. p. 169- 177.

Otegui MS. 2007.Endosperm: development and molecular biology. In: Olson OA, editor. Endosperm cell walls: formation, composition, and functions. Heidelberg (DE): Springer. p. 159178.

Proofs

Galey proof will be sent by email to correspondence author. The corrected proof should be returned within 5 working days to ensure timely publication of the manuscript.

Manuscript is sent to:

Website : www.ijop.id
E-mail : ijop.maksi@gmail.com

INTERNATIONAL JOURNAL of OIL PALM

ISSN: 2599-3496 print
ISSN: 2614-2376 online

sawit
BPDPKS